Global Biogeochemical Cycles®

Key Points:

- Unsupervised classification of 12 watershed types based on watershed properties predicts aspects of river hydrology and biogeochemistry
- Climate and topography create complex spatial mosaics of watershed types, streamflow regimes, and dissolved organic carbon dynamics
- Watershed classification for hydro-biogeochemistry may be useful for predictive mapping in other complex regions with sparse observations

Watershed Classification Predicts Streamflow Regime and Organic Carbon Dynamics in the Northeast Pacific Coastal Temperate Rainforest

Ian J. W. Giesbrecht[1,2] , Suzanne E. Tank[1,3] , Gordon W. Frazer[1,4], Eran Hood[5] , Santiago G. Gonzalez Arriola[1], David E. Butman[6] , David V. D'Amore[7] , David Hutchinson[8] , Allison Bidlack[5] , and Ken P. Lertzman[1,2]

[1]Hakai Institute, Vancouver, BC, Canada, [2]Simon Fraser University, Vancouver, BC, Canada, [3]University of Alberta, Edmonton, AB, Canada, [4]GWF LiDAR Analytics, Sidney, BC, Canada, [5]University of Alaska Southeast, Juneau, AK, USA, [6]University of Washington, Seattle, WA, USA, [7]Forest Service, U.S. Department of Agriculture, Juneau, AK, USA, [8]Water Survey of Canada, Vancouver, BC, Canada

Abstract Watershed classification has long been a key tool in the hydrological sciences, but few studies have been extended to biogeochemistry. We developed a combined hydro-biogeochemical classification for watersheds draining to the coastal margin of the Northeast Pacific coastal temperate rainforest (1,443,062 km^2), including 2,695 small coastal rivers (SCR) and 10 large continental watersheds. We used cluster analysis to group SCR watersheds into 12 types, based on watershed properties. The most important variables for distinguishing SCR watershed types were evapotranspiration, slope, snowfall, and total precipitation. We used both streamflow and dissolved organic carbon (DOC) measurements from rivers ($n = 104$ and 90 watersheds respectively) to validate the classification. Watershed types corresponded with broad differences in streamflow regime, mean annual runoff, DOC seasonality, and mean DOC concentration. These links between watershed type and river conditions enabled the first region-wide empirical characterization of river hydro-biogeochemistry at the land-sea margin, spanning extensive ungauged and unsampled areas. We found very high annual runoff (mean > 3,000 mm, $n = 10$) in three watershed types totaling 59,024 km^2 and ranging from heavily glacierized mountain watersheds with high flow in summer to a rain-fed mountain watershed type with high flow in fall-winter. DOC hotspots (mean > 4 mg L^{-1}, $n = 14$) were found in three other watershed types (48,557 km^2) with perhumid rainforest climates and less-mountainous topography. We described four patterns of DOC seasonality linked to watershed hydrology, with fall-flushing being widespread. Hydro-biogeochemical watershed classification may be useful for other complex regions with sparse observation networks.

Plain Language Summary Watersheds transfer large amounts of freshwater to the ocean, yet each watershed does this differently from the next. Geographic differences in climate and topography affect the global biogeochemical cycling of elements like carbon. However, most rivers in regions like the carbon-dense rainforest of western North America have no measurements of streamflow or carbon, making it hard to predict how river dynamics change across geographic locations. Our goal was to classify and map watershed types for an entire coastal region, with consideration of both water and carbon. Our results show the locations of watershed types with very different amounts and seasonality of runoff and of dissolved organic carbon (DOC). While we focused on DOC, these watershed types might naturally differ in other aspects of river biogeochemistry such as organic nitrogen and iron. Maps of watershed types should help society understand how land and sea are linked together over complex regions within a changing climate. However, certain watershed types have little or no long-term monitoring to guide climate adaptation. While many studies have classified watersheds from a hydrology perspective, few have considered carbon as well. Combining hydrology and biogeochemistry when mapping watershed types may be useful in other regions of the world.

1. Introduction

The movement of water and terrestrial material from land to sea is a critical biogeochemical process that influences estuaries (e.g., Arimitsu et al., 2018), the broader coastal ocean (Bauer et al., 2013; Carmack et al., 2015), and the global carbon cycle (Regnier et al., 2013). However, understanding of this process at a global scale is hindered by spatial heterogeneity and sparse observations. Indeed, key challenges in marine ecosystem ecology

include understanding the role of terrestrial and riverine export along the land-ocean aquatic continuum (Borja et al., 2020) and upscaling across complex spatial gradients (Xenopoulos et al., 2017). Many regions of the world lack a well-distributed network of empirical observation sites, hampering efforts to develop spatially generalizable models of watershed (catchment) processes and coastal exports (e.g., McClelland et al., 2015; Regnier et al., 2013). Under these conditions, the classification of watersheds may serve as a simple tool to extrapolate data and knowledge across extensive areas that remain unmeasured (Sivakumar et al., 2015). Watershed classification also offers a tool for summarizing diverse information in a simple and consistent form that improves communication, management applications, and conceptual development (e.g., Olden et al., 2012). In this study, we develop and test a deductive watershed classification (Olden et al., 2012), using the novel approach of a combined hydro-biogeochemical perspective (Covino et al., 2018; Li et al., 2021) and a regional scale data synthesis, for watersheds with a terminus along the margin of the Northeast Pacific Coastal Temperate Rainforest of North America (NPCTR).

Over the past two decades, the field of hydrology has pursued watershed classification intensively as a tool to organize and advance our understanding of dominant processes in the face of immense spatial complexity at regional to global scales (McDonnell & Woods, 2004; Sivakumar et al., 2015). One goal of watershed classification is to improve streamflow prediction in ungauged basins (Castellarin et al., 2011 special issue in HESS; Di Prinzio et al., 2011; Sivakumar et al., 2015; Smith et al., 2018). A broad and well-used framework for hydrologic classification was developed by Olden et al. (2012), based on a review of nearly 40 published examples. In this framework, deductive classifications are based on watershed characteristics expected to control streamflow, while inductive classifications are based on streamflow timeseries data, with the former being most useful in regions with sparse observations. New hydrologic classifications continue to emerge (e.g., Mosavi et al., 2021), including examples in portions of the NPCTR (e.g., Curran & Biles, 2021; Ouellet Dallaire et al., 2020; Sergeant et al., 2020).

Frameworks have also been developed to guide integrative "aquatic ecosystem classifications," which can consider aspects of aquatic biogeochemistry in the context of conservation planning and water quality management (Higgins et al., 2005; Melles et al., 2012, 2014, p. 549; Soranno et al., 2010). Water quality has been linked to local watershed classifications and regional zonation maps (Detenbeck et al., 2003; Greene et al., 2015; Larsen et al., 2017; Martin et al., 2011; Momen & Zehr, 1998; Soranno et al., 2010; Yu et al., 2015). For example, the Hydrologic Landscape Regions data set was developed to guide water quality assessment in the United States (Wolock et al., 2004) and has been evaluated with stream nitrogen and chloride data (Hoos & McMahon, 2009; Poor et al., 2008). Similarly, the River Environment Classification (REC) system developed in New Zealand (Snelder & Biggs, 2002) described river classes based on watershed climate, topography, geology, and landcover. The REC classes showed different levels of soluble reactive phosphorous, soluble inorganic nitrogen, and water clarity (Snelder & Hughey, 2005). In Chile, REC classes had different streamflow regimes and different levels of electrical conductivity (Peredo-Parada et al., 2011).

Several classification systems explicitly aim to represent the controlling factors of both hydrology and biogeochemistry during classification (e.g., Ouellet Dallaire et al., 2019; Snelder & Hughey, 2005; Wolfe et al., 2019; Wolock et al., 2004). However, most broad scale watershed classification studies we found evaluated the defined classes for streamflow regimes or for aquatic biogeochemistry but not both concurrently. We suggest that the fields of biogeochemistry and hydrology could both be advanced by further attention to watershed classification through the interdisciplinary lens of hydro-biogeochemistry (see Li et al., 2021).

Here we focus on two inter-connected aspects of freshwater runoff relevant to global biogeochemical cycling and land-sea linkages: streamflow regimes and dissolved organic carbon (DOC) concentrations. A streamflow regime can be described hydrologically in terms of magnitude, frequency, duration, timing, and rate of change and is widely considered a "master variable" that creates, maintains, and restores ecological integrity within river and floodplain ecosystems (Poff, 1996). Streamflow regimes can be mechanistically linked with watershed characteristics to indicate dominant hydrologic processes (McMillan, 2020; Roden, 1967; Sivakumar, 2004) such as the relative importance of rain, snow, and glacial contributions (Eaton & Moore, 2010; Trubilowicz et al., 2013). Importantly, spatial gradients in runoff magnitude and timing directly influence material fluxes and a number of physical and biological processes in the coastal ocean, at global (Milliman & Farnsworth, 2011; Syvitski et al., 2005), regional (e.g., Carmack et al., 2015; Cuevas et al., 2019), and local scales (e.g., Howe et al., 2017; Wetz et al., 2006). DOC and streamflow regimes are primarily controlled by the same processes and watershed

characteristics (climate and glaciers, topography, soils, and vegetation), even if the relationships differ (e.g., Edwards et al., 2013).

While we are interested in river biogeochemistry in general, we focus our analysis on DOC for several reasons. First, DOC links the ecology of carbon-dense regions, such as the NPCTR (McNicol et al., 2019), with the ecology of the sea. For example, fluvial export of terrestrially derived dissolved organic matter (DOM; including DOC) stimulates heterotrophic production (St. Pierre et al., 2020) and foodweb uptake (Arimitsu et al., 2018; Hitchcock et al., 2016). Second, the threat of global climate change to human societies motivates a need to better understand lateral fluxes within the carbon cycle (Bauer et al., 2013; Fellman et al., 2017; Regnier et al., 2013; Zarnetske et al., 2018). Third, the NPCTR is a DOC export hotspot in the global context (Edwards et al., 2021; Hood et al., 2009; Mayorga et al., 2010; Oliver et al., 2017), yet has wide ranging spatial variation in DOC concentrations (D'Amore et al., 2016) and seasonality (Fellman et al., 2014; Oliver et al., 2017). Finally, watershed classification that successfully predicts DOC concentrations and seasonality may also be useful for other biogeochemical variables with similar landscape controls such as dissolved organic nitrogen and iron (Kritzberg et al., 2014; Schroth et al., 2011; St. Pierre et al., 2021; Sugai & Burrell, 1984).

Watershed classification may further our understanding of the coupling of DOC dynamics with watershed hydrology over complex spatial gradients. After analyzing seasonal DOC and streamflow dynamics spanning the geography of Sweden, Winterdahl et al. (2014) proposed four watershed classes, characterized by: (a) flow driven DOC concentration dynamics (in catchments where higher flows access more soil organic matter); (b) temperature driven DOC dynamics (in small peat dominated catchments); (c) flow and temperature driven DOC dynamics with a spring peak from snowmelt (in cold catchments); (d) non-seasonal DOC dynamics unrelated to flow or temperature (large catchments or large lake cover). Across the Conterminous United States (CUS), Zarnetske et al. (2018) found the degree of transport limitation of DOC flux varied with local watershed characteristics (e.g., wetland cover) but not ecoregional classes.

The NPCTR margin is an ideal test region for hydro-biogeochemical watershed classification, known for high yields of water (e.g., Edwards et al., 2021; Morrison et al., 2012; J. Wang et al., 2004) that influence ocean ecosystems (e.g., St. Pierre et al., 2021) and regional carbon cycles (Butman et al., 2016; Stackpoole et al., 2017). It is also a region undergoing rapid ecosystem change due to warming temperatures, extremely high rates of glacial retreat (Clarke et al., 2015; O'Neel et al., 2015), and changing streamflow regimes (Bidlack et al., 2021; Shanley et al., 2015). Yet the region is physiographically complex (Church & Ryder, 2010) and most watersheds remain ungauged and unsampled. While there is gauging on the 10 large continental watersheds (Figure S1 in Supporting Information S1), which have been conceptualized as *point sources* of runoff to the ocean, small coastal rivers (SCR) collectively can be thought of as a major *line source* that is sparsely represented in the current gauging network (Royer, 1982; J. Wang et al., 2004). A unified high-resolution watershed classification map has yet to be developed for the entire NPCTR margin, including both SCR and continental rivers and both northern (Perhumid) and southern (Seasonal) areas of the rainforest (Figure S1 in Supporting Information S1).

We have two main goals with this work: (a) Develop and evaluate a practical deductive method for defining and mapping broad classes of river hydro-biogeochemistry in regions with sparse observational networks; (b) Develop a new spatially explicit conceptual model of watershed biogeochemistry (DOC) and hydrology for the coastal margin of the NPCTR. We begin by defining watershed types based on watershed characteristics before comparing them in terms of four aspects of river hydro-biogeochemistry: streamflow regimes, mean annual runoff, DOC seasonality, and mean DOC concentrations. We hypothesize that these measures of river hydro-biogeochemistry correspond with catchment-based watershed types, reflecting underlying controls by climate, topography, soils, and vegetation.

2. Methods

2.1. Study Area Description

Our study area (1,443,062 km^2, Figure S1 in Supporting Information S1) covers all land draining to the coastal ocean between approximately Skagway, Alaska (AK) and the Russian River in California (CA). This region corresponds to the portion of the North American coastline where the temperate perhumid rainforest (north of Knight Inlet/Vancouver Island) and seasonal coastal rainforest (from Vancouver Island southward) dominate (Alaback, 1996; Wolf et al., 1995). Rainforest ecosystems dominate the westernmost 30–250 km of the continent

due to the strong orographic effect of the coastal mountains on precipitation from Pacific air masses, with the greatest precipitation in fall and winter months (Lane et al., 2018; Morrison et al., 2012; Royer, 1982). Inland of the coastal mountains lies a vast area of plateaus and inland mountains with continental climates, which range from boreal and alpine tundra in the north, through hemiboreal, to arid steppe and desert in the south (Beck et al., 2018). Extensive glaciers are found in coastal ranges of AK and British Columbia (BC), with lesser amounts of glacial ice cover in the Rocky Mountains and coastal mountains of the CUS (RGI Consortium, 2015). North of approximately the Puget Sound drainage basin, the landmass was covered by the Cordilleran ice sheet during the Pleistocene (Menounos et al., 2009), contributing to a high degree of physiographic complexity (e.g., glacial troughs, fjords, island archipelagos, and large depositional landforms that now form coastal lowlands; Church & Ryder, 2010). Ten large continental watersheds drain the majority (78%) of the study area, spanning both continental and coastal areas, whereas thousands of smaller (i.e., SCR) watersheds drain the coastal rainforest.

2.2. Watershed Delineation

Watershed polygons were taken from Gonzalez Arriola et al. (2018), who merged existing watershed boundary data sets from three jurisdictions (AK, BC, and CUS), resulting in the highest resolution watershed mapping ($\sim$20 km^2 minimum catchment size) available at a consistent scale across the region. Prior to analysis, we omitted 62,711 very small polygons (<10 km^2) which together represent only 0.27% of the region yet would otherwise have a disproportionately large influence on the cluster analysis due to their great abundance. The omitted polygons (mean size 0.06 km^2) were mostly tiny islets and other emergent, offshore rock outcrops. The resulting data set contains 2,708 watershed polygons (99.73% of the region), with 94.4% of the area in individually delineated watersheds (mean 1,207 km^2) and 5.6% of the area in polygons that represent amalgamations of multiple adjacent small streams (mean 52 km^2).

2.3. Watershed Characteristics

We identified topographic, climatic, land cover, and geographic variables expected to represent the key watershed-controls on stream hydro-biogeochemistry (Figure 1; Table 1). This list of variables was supported by a review of known controlling factors (e.g., Aitkenhead-Peterson et al., 2005; Eaton & Moore, 2010; Fleming, 2005; Hood & Berner, 2009; Mulholland, 2003; Trubilowicz et al., 2013) and the success of other watershed classifications (e.g., Ouellet Dallaire et al., 2019; Snelder & Hughey, 2005; Wolock et al., 2004; see Table S1 in Supporting Information S1 for detailed rationale). Several other variables such as May-to-September (MSP) precipitation, % precipitation as snow, and % lake cover were computed, evaluated, and used to aid interpretation, but were not included in the final cluster analysis. For this analysis, we did not attempt to quantify human-alteration of watersheds, yet acknowledge widespread watershed alteration, particularly in the southern half of the region (Wolf et al., 1995).

All candidate variables were calculated from published geospatial datasets that were freely available, peer-reviewed, and spatially consistent across all three geopolitical regions with respect to variable definitions and estimation approaches (Table S1 in Supporting Information S1). We extracted basic watershed-level statistics (i.e., mean, maximum, or proportional values) for each selected variable by overlaying the watershed boundaries on the associated source data layer. The final data set had 2,705 polygons after omitting three polygons with suspect or missing attribute data. For slope, vegetation, and glacier cover metrics, summary statistics were computed for the portion of the watershed that did not include lakes.

2.4. Watershed Classification

We used two separate approaches to place all watersheds into discrete types. First, we set aside 10 large continental watersheds (Figure S1 in Supporting Information S1) because we expected them to be fundamentally different from the SCR watersheds (e.g., Bidlack et al., 2021) in terms of catchment controls on river hydro-biogeochemistry (e.g., watershed size, transit times, groundwater storage, agricultural land use, and fluvial network structure are likely of increasing importance). Second, we grouped the remaining 2,695 SCR watersheds into statistically similar clusters using k-means partitioning (Hastie et al., 2009) with 12 variables and 12 clusters, after exploring several permutations of different statistical clustering methods (k-means, k-medoids, unsupervised random forest), different lists of input variables, and different numbers (k) of clusters (Figure 1). The list of input variables

Figure 1. A general workflow for deductive watershed classification and validation for a combined hydro-biogeochemical perspective on riverine conditions and dynamics. Notes on the right offer additional detail, options, examples, or specifics from this study (e.g., k-means statistical clustering algorithm).

p was refined to represent a range of known catchment controls on hydro-biogeochemistry (e.g., climate and topography) while minimizing the correlations among variables. The number of clusters k was determined in part using the rate and pattern of decline in the within-cluster sum of squares with increasing k (Figure S2 in Supporting Information S1). The final k-means clustering with $p = 12$ and $k = 12$ was judged to best reflect known biophysical patterns previously described by regional map products, such as a global climatic classification (Beck et al., 2018), ecoregions of North America (CEC, 2009), physiographic provinces (e.g., Church & Ryder, 2010 in BC), rainforest zones (Wolf et al., 1995), glacier cover (RGI Consortium, 2015), and Biogeoclimatic Ecosystem Classification in BC (Salkfield et al., 2016). We used principal component analysis (PCA), ordination biplots, and contour plots (Figure S3 in Supporting Information S1) to visualize aspatial relationships among watersheds and watershed groups. All input variables were scaled to zero mean and unit variance prior to k-means partitioning and PCA.

Table 1
Mean (and Standard Deviation) of the 12 Watershed Properties Used for Clustering Analysis

Watershed type	Centroid x location Poly_x	Centroid y location Poly_y	Glacier cover (%) Glc_prct	Max elev (m) Elev_max	Slope (°) Slpe_avg	Slope <5° (%) Slpe5	MAP (mm) MAP_avg	Eref (mm) Eref_avg	PAS (mm) PAS_avg	MAT (°C) MAT_avg	TD (°C) TD_avg	Veg height (m) VegHt_avg	Area (km²) Area_km2	Polygons (N) Poly_n
GMH	−2207041	2613545	62.840	2,627	17.8	26.3	4,755	298	2,851	0.17	15.74	0.9	384	41
	(87619)	(187570)	(13.486)	(730)	(4.4)	(14.8)	(1,399)	(31)	(886)	(1.17)	(1.47)	(1.7)	(326)	
GMM	−2077757	2266114	11.652	1,877	26.3	4.6	3,192	384	1,533	2.05	16.58	7.3	327	178
	(93153)	(361800)	(8.675)	(402)	(3.4)	(4.1)	(892)	(43)	(428)	(0.92)	(1.09)	(5.5)	(831)	
SMX	−2233795	2538454	1.282	1,113	22.5	6.7	4,145	371	1,212	3.59	13.82	9.1	54	197
	(46007)	(90396)	(3.267)	(226)	(3.9)	(6.4)	(1,158)	(16)	(324)	(0.76)	(1.15)	(5.1)	(39)	
SMN	−2069437	2036404	0.131	1,146	24.8	3.8	4,433	461	1,106	4.85	15.53	23.5	58	314
	(33773)	(171446)	(0.502)	(247)	(3.5)	(2.7)	(708)	(34)	(302)	(0.87)	(0.97)	(3.4)	(55)	
SMC	−1941546	1625420	0.787	1,781	26.0	4.3	2,722	513	736	5.10	15.40	24.2	278	248
	(66158)	(243028)	(1.851)	(407)	(4.5)	(6.7)	(540)	(47)	(256)	(1.20)	(1.10)	(4.5)	(925)	
RMN	−2195221	2347359	0.002	806	17.1	12.6	3,085	417	566	5.15	13.30	22.0	50	516
	(55354)	(190728)	(0.023)	(171)	(3.3)	(7.1)	(626)	(27)	(175)	(0.82)	(1.16)	(3.6)	(66)	
RHN	−2181865	2208147	0.000	544	9.6	32.8	2,720	441	291	6.29	12.32	20.6	50	329
	(59700)	(231836)	(0.000)	(204)	(2.5)	(12.0)	(504)	(32)	(102)	(0.78)	(1.00)	(3.4)	(58)	
RLN	−2161232	2046325	0.000	230	3.6	76.5	2,278	468	150	7.12	11.39	18.5	46	138
	(70023)	(281377)	(0.000)	(164)	(1.5)	(14.6)	(568)	(40)	(71)	(0.90)	(1.12)	(3.6)	(49)	
RMC	−2037953	1574117	0.017	1,087	21.1	8.1	3,794	553	386	7.11	12.78	27.9	96	261
	(46094)	(156730)	(0.204)	(304)	(4.3)	(5.8)	(618)	(42)	(159)	(0.76)	(1.13)	(2.7)	(177)	
RHC	−1956121	1373649	0.000	787	10.9	26.5	2,126	626	131	8.45	12.85	25.8	157	227
	(64923)	(189085)	(0.000)	(372)	(3.4)	(13.0)	(673)	(63)	(79)	(0.80)	(1.65)	(3.3)	(463)	
RLC	−1903634	1213933	0.000	254	4.3	68.2	1,366	702	40	9.79	12.35	19.0	64	158
	(63158)	(139889)	(0.000)	(189)	(1.8)	(16.6)	(550)	(56)	(23)	(0.55)	(1.71)	(5.3)	(56)	
RHS	−2165234	488409	0.000	729	12.3	19.4	1,802	895	22	11.34	9.28	26.8	304	88
	(56393)	(228072)	(0.000)	(351)	(4.1)	(17.1)	(531)	(107)	(16)	(0.86)	(1.85)	(4.6)	(608)	
SC	−1851232	2004722	3.918	3,074	14.4	26.6	1,139	461	608	1.63	20.29	14.1	174,934	6
	(195414)	(598574)	(3.283)	(624)	(2.6)	(9.6)	(258)	(156)	(243)	(2.37)	(1.18)	(3.8)	(256,810)	
RC	−2079102	520528	0.001	3,010	13.3	19.8	1,329	977	76	10.15	15.63	27.0	18,922	4
	(67869)	(159221)	(0.003)	(863)	(1.5)	(13.2)	(250)	(66)	(32)	(1.41)	(1.71)	(3.7)	(14,562)	

Note. This table also reports mean watershed area and total number of polygons. Acronyms for watershed types are defined in Figure 2. A horizontal line divides the 12 SCR watershed types from the two continental watershed types. The variables were defined as follows: Glc_prct = % cover of glaciers; Elev_max = maximum watershed elevation; Slpe_avg = average watershed slope; Slpe5 = the proportion of the watershed with slope <5°; MAP_avg = Mean Annual Precipitation; PAS_avg = Precipitation As Snow; MAT_avg = Mean Annual Temperature; TD_avg = Temperature Difference between mean warmest month temperature and mean coldest month temperature (a measure of continentality); Eref_avg = Hargreaves reference (potential) evapotranspiration; VegHt_avg = mean vegetation height; Poly_x and Poly_y indicate watershed centroid coordinates. All climate variables were calculated as the mean of grid cells located in a watershed.

2.5. Variable Importance

We used supervised random forest (RF) classification, variable importance, and feature selection to determine which clustering variables provided the most discriminatory power in the separation of SCR watershed types (Table S2 in Supporting Information S1). We selected two unique, yet complementary measures of variable importance. First, we used mean minimal depth to determine the average depth at which a predictor first appeared as a splitting variable beneath the root node. Splitting variables found closer to the root node are generally considered more important than those found further down in the tree (Ishwaran, 2007). Second,

both raw and scaled permutation were used to estimate the average increase in out-of-bag (OOB) classification error that occurred when the relationship between a predictor and response was disturbed by random shuffling (Breiman, 2001). We also employed two backward, feature selection strategies, known as non-recursive (NRFE) and recursive feature elimination (RFE) to identify a subset of variables most effective in predicting watershed type (Gregorutti et al., 2017; Guyon et al., 2002). Finally, we created separate model performance curves, with the number of variables on the abscissa against the OOB classification error on the ordinate, to determine which combination of variable importance and feature selection strategy produced the best rank ordering of variable importance. We used 200 randomizations of rank variable importance and NRFE to establish a mean baseline performance curve for the unusual case where there was no logical ordering of variable importance among predictors. We omitted geographic coordinates (of watershed centroids) from these analyses of variable importance, because (a) they were difficult to interpret and contributed limited explanatory power to the RF model (i.e., the OOB error rate increased from 5.1% to 6.1% when Poly_x and Poly_y were excluded); (b) Poly_y was strongly correlated with Eref ($r = -0.9$) and moderately correlated with Poly_x ($r = -0.7$), and thus had the potential to distort and obscure the true rank ordering of the most functionally relevant variables (Nicodemus et al., 2010).

2.6. Discharge

Discharge data were acquired for near-outlet gauging stations in 104 independent watersheds, after omitting stations that were obviously unrepresentative of the watershed polygon used for classification (e.g., the Lemon Creek gauge near Juneau, AK, is located in a subcatchment with much greater glacier cover than the overall watershed) and stations of short duration (<5 years) or poor quality (e.g., seasonal data only; see gauge list in corresponding data package for site assessment notes; Giesbrecht et al., 2022). Discharge values were acquired for the period 1981-01-01 to 2010-12-31, as available. While longer records (e.g., 15 years) and greater record overlap (e.g., 50%) produce more stable streamflow metrics, in data sparse regions the "best use of the available data must be made" (Kennard et al., 2010, p. 150).

We considered all gauges operated by the Water Survey of Canada (WSC) and the US Geological Survey (USGS). We included both active and deactivated gauges to increase spatial coverage. Where multiple gauged rivers converge near a common outlet, we used the summed flow and summed area of all gauges. Our search of USGS gauges was based on the "*GAGES-II*" inventory of Falcone (2011), which notably omitted a gauge on the lower Skagit River. We used R to access and integrate daily discharge data from the two national databases. This required the "*tidyhydat*" package for WSC and "*dataRetrieval*" package for USGS. We omitted leap days (February 29) due to smaller sample sizes (e.g., Curran & Biles, 2021). Specific discharge was calculated as the mean daily flow in $m^3 \, s^{-1}$ divided by the gauged drainage area in km^2. We assigned streamflow regimes to one of five archetypes known for this region, based on the work of Eaton and Moore (2010) and Trubilowicz et al. (2013). Mean annual runoff (MAR) was calculated as the sum of mean daily runoff values.

2.7. Dissolved Organic Carbon

We compiled a data set of 4,546 riverine DOC concentration ($mg \, L^{-1}$) measurements at near-outlet stream locations in 90 watersheds. We omitted sites that were clearly unrepresentative of the watershed outlet (e.g., located in a headwater stream or a nested catchment with much lower/higher slope than the watershed polygon) and sites with suspect data quality (e.g., persistent values of 1.0 at Cummins Creek, OR. See DOC site list in corresponding data package for site assessment notes; Giesbrecht et al., 2022). Additionally, we omitted sites with $n < 5$ samples, except in the case of four watershed types that would otherwise have <5 polygons with data. In these cases, we accepted sites with $n \geq 3$ samples. In watersheds with multiple sites, we either selected the most representative station (e.g., a mainstem site) or averaged data from multiple stations to achieve representation of the polygon (e.g., multiple small streams draining from an amalgamated polygon). The DOC sites did not necessarily correspond with the gauging locations. Accepting sites without both data types allowed us to maximize the spatial coverage of validation data.

The DOC data set was derived from an exhaustive search of six different water-quality databases. For river outlets in the USA, we downloaded data from four databases (e.g., EPA and USGS) using the Water Quality Portal (WQP) Data Discovery Tool in R for the time period 1981-01-01 through 2019-09-30. Environment and Climate Change Canada provided a spreadsheet of DOC data upon request (ECCC, 2019). From this data set we omitted records from the San Juan and Fraser Rivers with high specific conductance (>100 μs/cm),

which is indicative of seawater mixing at these tidally influenced sampling sites (personal communication, Ayisha Yeow ECCC). To increase the spatial coverage in more remote watersheds of British Columbia, we included DOC samples from the Hakai Institute's database of coastal watershed biogeochemistry (see Tank et al., 2020 for lab methods).

2.8. Sensitivity Analysis

Given the sparse observation network in parts of this region, we included all the gauging stations and DOC sampling sites that met basic criteria for location, temporal coverage, and quality (Figure 1). This meant accepting some sites with significant anthropogenic alterations or other factors (e.g., small sample size) that might affect stream hydro-biogeochemistry results. However, we assessed the sensitivity of our main results (e.g., plots of streamflow and DOC) to the inclusion or omission of these sites (see site ranking in Giesbrecht et al., 2022) and found the main conclusions were not impacted except by improving data coverage in some watershed types. This analysis was not designed to evaluate anthropogenic impacts on stream hydro-biogeochemistry.

2.9. Contour Plots

We constructed contours of predicted MAR and DOC within the first two dimensions of PCA ordination space using two separate training datasets of observed MAR and DOC collected for a subset of watersheds. Predictions were derived from Generalized Additive Models (GAM) of the form $y = \alpha + f_1(x_1, x_2) + \varepsilon$, where $f_1(x_1, x_2)$ is a two-dimensional isotropic smooth function, which describes the interaction between predictors x_1 and x_2 on the response y; x_1 and x_2 are respectively the first two principal components (PC1 and PC2) of the PCA. Both prediction models were fitted by the R package "*mgcv*" V1.8-31, using the gamma family of distributions and log-link function to constrain the predicted response to positive values. Smoothing parameters were automatically selected using the restricted maximum (REML) likelihood method. Out-of-sample (generalization) prediction errors were estimated using mean goodness-of-fit statistics (i.e., adjusted R^2 and the percent deviance explained) obtained from repeat (10 times) 10-fold cross validation.

2.10. Calculation of Regional Totals

We assessed the area-weighted importance of each watershed type. To do this, we calculated the absolute and relative contribution of each watershed type to the total regional area, total mean annual precipitation, total mean annual precipitation as snow, and total glacial ice cover. For precipitation, we calculated the mean annual volume of water inputs to each watershed as the product of watershed area and watershed-mean precipitation. We then summed the total precipitation volume of all watersheds in each type and for the entire region. For glaciers, we summed glacier cover across all watersheds in each type and in the region. We then calculated the relative (%) contribution of each watershed type to regional total areas (watershed area and glacier area) and volumes (precipitation and precipitation as snow).

3. Results

3.1. Watershed Types and Distinguishing Watershed Characteristics

The cluster analysis grouped the 2,695 SCR watersheds into 12 distinct watershed types, with most of the variance among watersheds explained by two principal components (Figure 2). The 12 SCR watershed types were given three-letter labels reflecting the characteristic water source, topography, and a modifier (Figure 2, Table 1). This approach to labeling represents the statistically important variables, easy-to-remember distinguishing features (e.g., latitudinal zone, glacier cover), and known catchment controls on runoff and DOC (e.g., glacier cover). Outside the SCR zone, two continental watershed types were recognized by visual inspection of the data (Table 1) and labeled by the characteristic water source alone (SC—Snow Continental and RC—Rain Continental).

Analysis of variable importance showed that three of the clustering variables—Eref, Slpe_avg, and PAS (Table 1)—accounted for most of the discriminatory power (Table S2 and Figure S2b in Supporting Information S1) in the separation of watershed types (Figure 2). Eref had a strong positive correlation with MAT ($r = 0.9$) and negative correlation with latitude (Poly_y; $r = -0.9$; Figure 2; Figure S2c in Supporting Information S1), which together suggested a broad thermal gradient from north to south (hence the *latitude* modifier). Mean slope
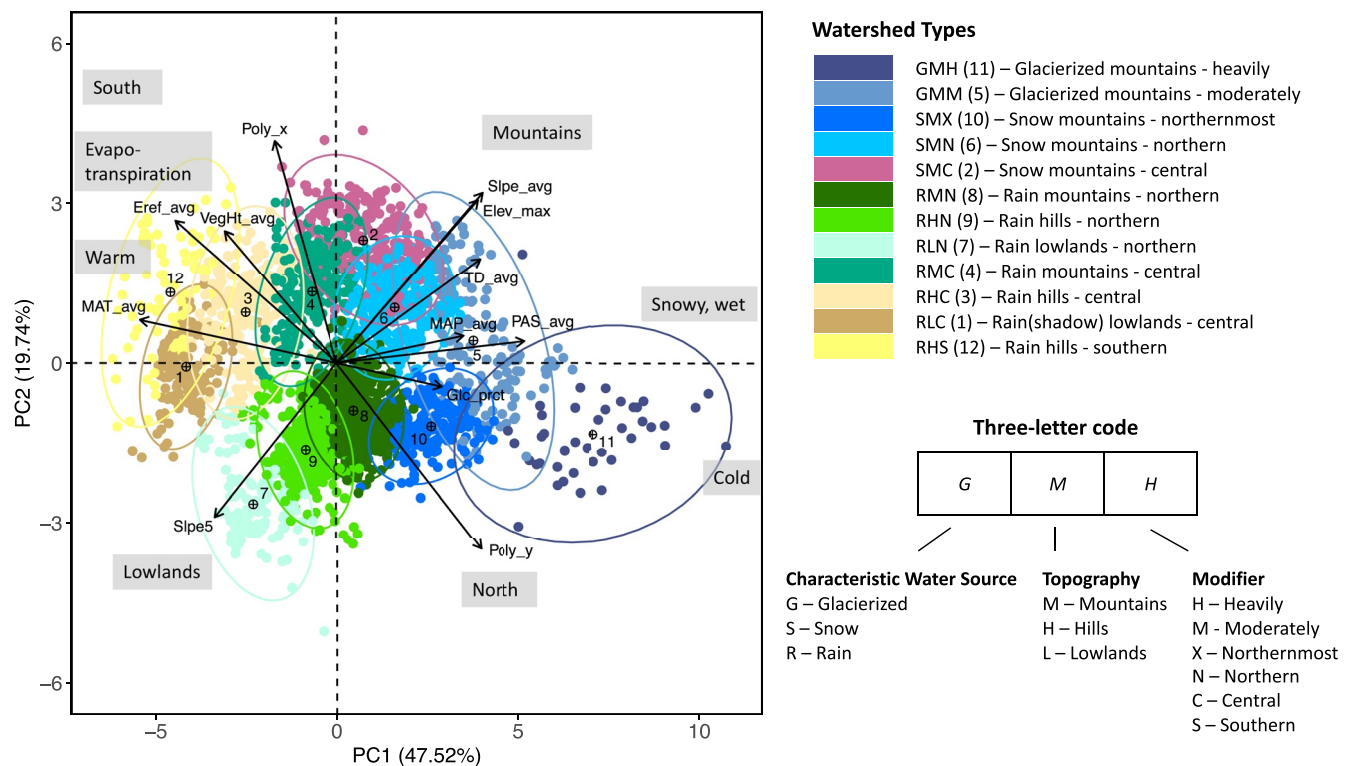
Figure 2. Ordination bi-plot of principal components 1 and 2, showing clustering results for SCR watersheds. Each point represents a watershed, while colors denote the $k = 12$ watershed types, each labeled with a three-letter code. Vectors show the direction and strength of correlation between individual watershed properties ($p = 12$) and the PCs. Cross-hairs mark the geometric center (centroid) of the corresponding cluster, labelled by cluster ID number. For each cluster, the ellipse delineates the 95% probability contour of a bivariate normal distribution (PC1 and PC2). Gray text boxes offer interpretative labels for generalized regional gradients in climate and topography. The legend is respectively ordered by characteristic water source, latitudinal modifier, and topographic group, in that order.

was correlated with relief (Elev_max; $r = 0.7$) and described a topographic gradient from flat-lowland watersheds to steep-mountainous watersheds (hence the *topography* code), broadly oriented with continentality. PAS was correlated with cold temperatures (MAT; $r = -0.8$) and heavy glacier cover ($r = 0.6$; Figure S3 in Supporting Information S1) and thus represented a gradient from cold and glacierized watersheds to warm and rain dominated watersheds (hence the *water source* code). The fourth strongest predictor of watershed type was MAP; however, in contrast to the top three ranked predictors, MAP occurred much lower in the ensemble of decision trees (Table S2 in Supporting Information S1). We therefore suspect that MAP interacted with thermal and topographic gradients to produce the spatial mosaic of watershed characteristics in this region.

The SCR and continental watersheds when combined represented 14 watershed types, each of which can be mapped (Figure 3) and described in terms of typical watershed properties and internal variability (Table 1, Figure S4 and Text S1 in Supporting Information S1). For example, GMH represented the mountainous ($2,627 \pm 739$ m elevation) and cold ($0.17° \pm 1.17°C$) extreme for the region, with correspondingly extreme ice cover ($62.8 \pm 13.5\%$), MAP ($4,755 \pm 1,399$ mm), PAS ($2,851 \pm 886$ mm, $60.7 \pm 9.9\%$), and (low) mean vegetation height (0.9 ± 1.7 m). RHS represented the warmest watersheds in the region (MAT $11.34° \pm 0.86°C$), with the highest evapotranspiration on the coast (895 ± 107 mm), spanning from the central coast of Oregon to northern California. The three-letter labels can also be used to group the watershed types by water source or terrain (Figure 2, Figure S5 in Supporting Information S1), creating a nested classification mapping system.

3.2. Streamflow Regimes Across Watershed Types

We hypothesized that the statistical clustering based on watershed properties would yield coherent watershed types with predictable streamflow regimes. Indeed, mean streamflow regimes showed clear association with watershed types and varied dramatically across the coastal region (Figure 4). Some watershed types also contained substantial internal variation related to the defining characteristics of the type (combinations of PAS, glacier cover, and
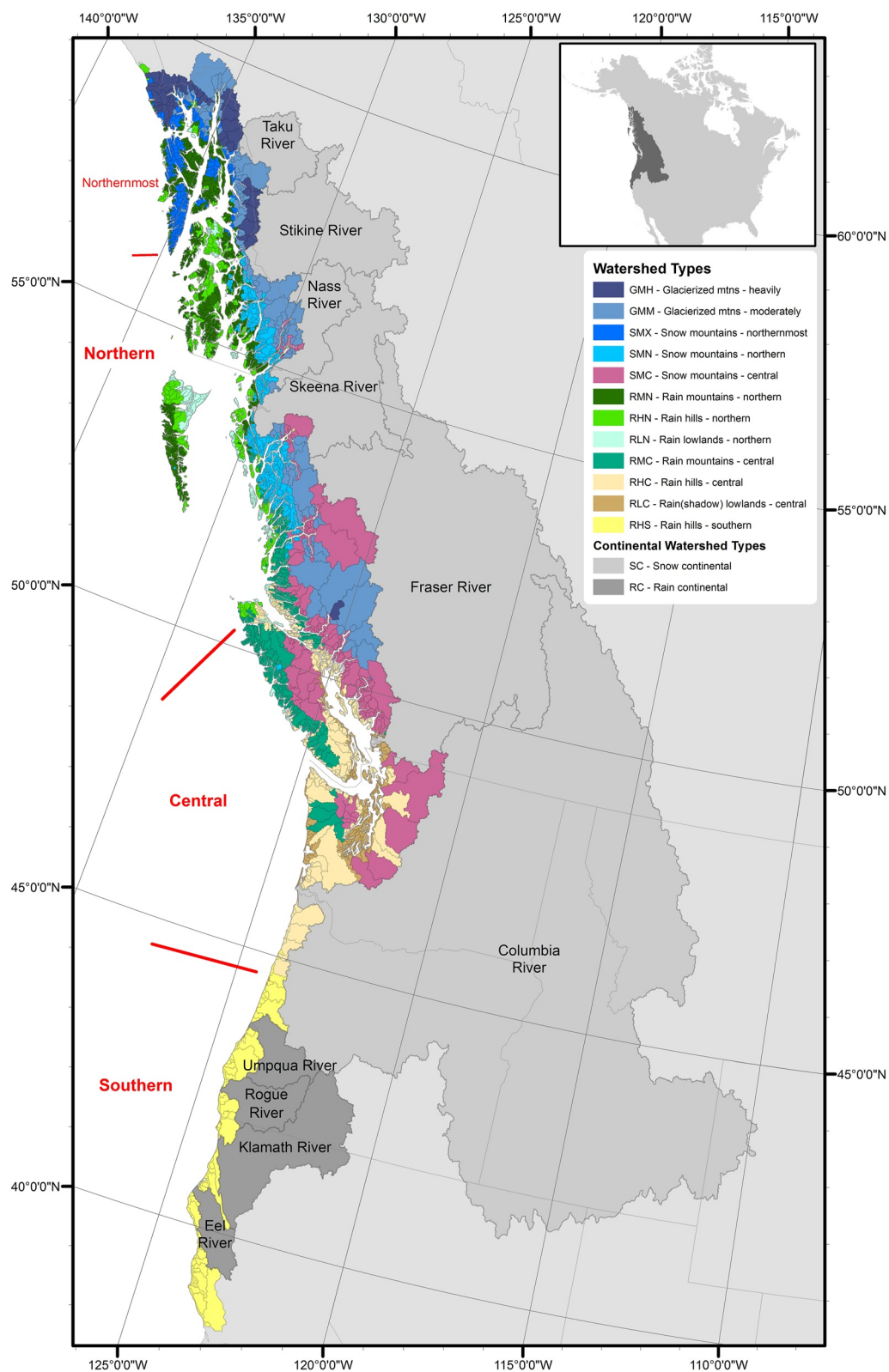
Figure 3. Map of the 14 watershed types of the NPCTR margin, ranging from heavily glacierized mountains (GMH) in the north to rain hills in the south (RHS) to two large continental watershed types draining inland areas (SC and RC).
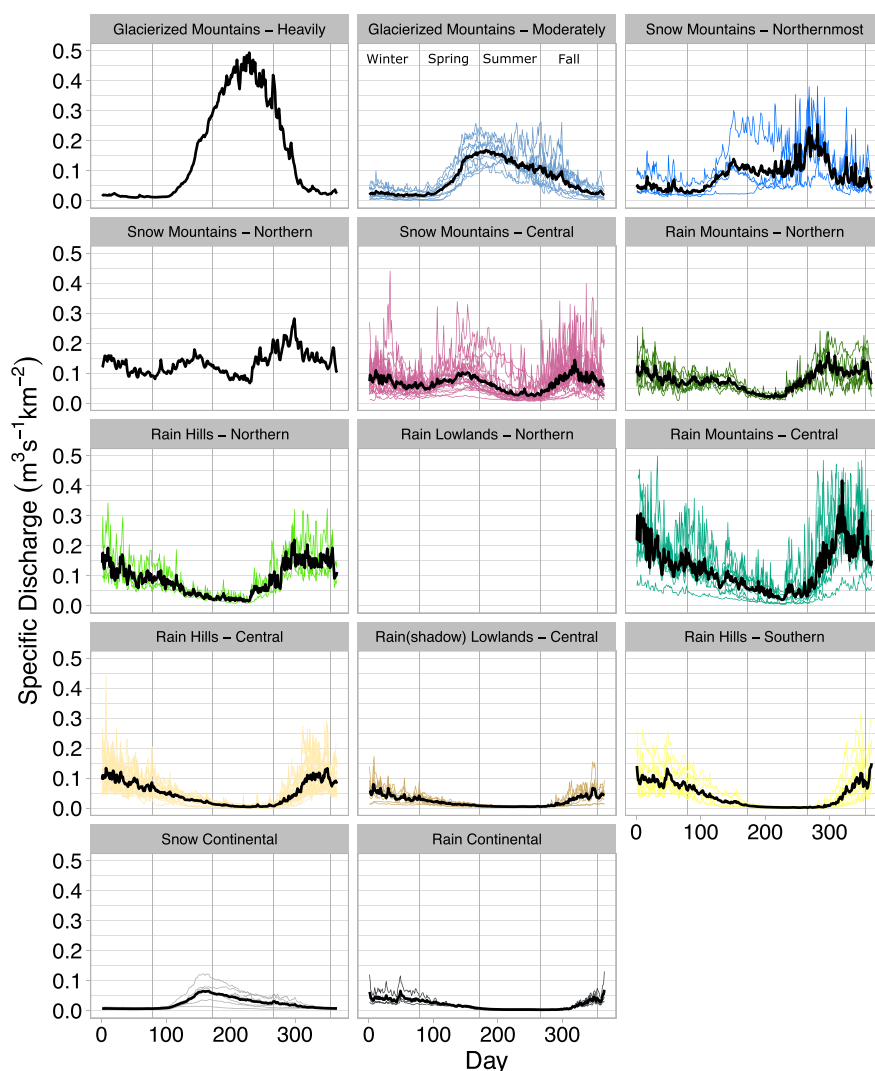
Figure 4. Observed streamflow regimes by watershed type summarized for all 104 gauged watersheds. Specific discharge was calculated for each watershed as a daily mean between 1981 and 2010, based on available data. Heavy black lines represent the mean specific discharge observed across watersheds of a type. Thin colored lines represent the specific discharge observed in gauged watersheds and indicate the degree of within-type spatial variation. Extreme values (0.5–0.9) observed at two RMC gauges are not shown, to improve the resolution of this figure. The number of gauged watersheds per watershed type varied from 0 in RLN to 22 in SMC (see Table 2). Vertical reference lines mark the divisions between the four astronomical seasons.

MAP in particular; Text S2 in Supporting Information S1). In the SMC type, for example, the spring freshet was more pronounced in watersheds with high PAS and low glacier cover. In SMC and GMM types, watersheds with higher glacier cover reached maximum summer flow later, reflecting a shift from snowmelt to icemelt controlled runoff timing (Fleming, 2005) and potentially also reflecting the effect of elevation on snowmelt timing and summer precipitation (Curran & Biles, 2021). Due to such catchment level controls, the SMC type included a few watersheds with the *nival dominant hybrid* or *glacier supported nival* streamflow regimes defined by Eaton and Moore (2010) and Trubilowicz et al. (2013), while the *pluvial dominant hybrid* regime was most common across the 22 gauged watersheds. Importantly, the variation within watershed types was generally small relative to the variation between most types, in terms of general hydrograph shape (timing and duration of high and low flow periods). As such, the mean discharge hydrograph for each watershed type provided a simple but useful tool to describe broad streamflow patterns across the region.

Five of the SCR watershed types had mean streamflow regimes clearly influenced by snowmelt, with varying degrees of glacial influence (Figure 4). *Glacial* and glacier supported nival streamflow regimes (Eaton & Moore, 2010; Trubilowicz et al., 2013) were found in the two glacierized watershed types (GMH and GMM, respectively). The GMM average hydrograph peaked in the spring/early summer whereas the snowier and more heavily glacierized GMH peak was later and much larger. The three snow-mountain watershed types (SMX, SMN, and SMC) had mean hydrographs that were characterized by two high flow periods: high flows in spring associated with snowmelt and higher flows in fall associated with fall rains. As such, all three typically had the pluvial dominant hybrid streamflow regime defined by Eaton and Moore (2010) and Trubilowicz et al. (2013), although fall flows were not much higher than spring flows in the SMC type. Watershed types SMX and SMN maintained relatively high flows in mid-summer despite generally low glacial cover (0%–3%), likely reflecting the combination of high summer precipitation (MSP > ~1,200 mm on average), high annual snowfall (>~1,000 mm on average), low evapotranspiration, and glacial contributions in some watersheds. By contrast, SMC had much lower summer flows, likely reflecting the more southerly climate. Watershed types SMC and SMN showed sustained winter flows due to ongoing rain at lower elevations whereas cluster SMX had relatively low winter flows reflecting a colder climate with a greater proportion of precipitation as snow at all elevations.

Of the remaining six SCR watershed types, the five that had streamflow data all showed a predominantly rain-driven (*pluvial;* Eaton & Moore, 2010; Trubilowicz et al., 2013) mean hydrograph ($n = 57$ gauged watersheds), despite snowmelt contributions in some gauged watersheds (Giesbrecht et al., 2022). Each rain watershed type had a distinct seasonality that reflected watershed climate and latitude. Fall flows increased earlier in the north and later in the south, similar to the pattern observed by Eaton and Moore (2010) within BC specifically. Mean hydrographs of the RMN, RHN, and RMC types reflected a wet, rain-dominated climate: high flows in fall and winter, followed by early/mid-summer low flows, and increasing flows by late summer. RMN had the most stable spring flows on average, likely because it received the most snow and two of the gauged watersheds had spring freshets. RMC was distinguished by the highest fall and winter flows in the region and a short low flow period, reflecting the extreme rainfall of this watershed type. In rainshadow and more southerly locations, RHC, RLC, and RHS had consistently much lower and longer summer low flows reflecting a lack of significant snowmelt, low seasonal precipitation (MSP < 500 mm), and high evapotranspiration. Fall through winter flows decreased from RHC to RHS to RLC watershed types, corresponding with decreasing MAP. The two driest types (RLC and RHS) did not experience rising flows until mid-fall. The coastal rainshadow type (RLC) had a streamflow regime very similar to the RC type of the Southern zone. RLN did not have a gauge yet catchment characteristics (MAP, Eref, and % snow) suggest a streamflow regime that is similar to RHN, but with lower runoff magnitude.

The 10 continental rivers showed either snow-dominated or rain-dominated streamflow regimes (Figure 4). In the SC watershed type, mean runoff was highest in late spring and slowly receded through summer. This *nival* streamflow regime reflected the high proportion of precipitation as snow (mean 52%) in this watershed type. Among the six SC watersheds, the three northernmost rivers (Taku, Stikine, Nass) had the most prolonged summer flows (Figure S6 in Supporting Information S1), which corresponded with higher glacial cover (5.9%–7.5% vs. 0.3%–1.5% in the Skeena, Fraser, and Columbia) and more snow (750–859 mm vs. 251–581 mm; 54%–66% vs. 34%–46%), suggesting a glacier supported nival runoff regime. The SC watersheds also had a higher ratio of MSP to MAP than most watershed types, suggesting additional rainfall contributions to summer flows. A secondary period of rain induced flows was evident in all SC watersheds in fall. The importance of atmospheric rivers on these continental watersheds (e.g., Curry et al., 2019) was likely underestimated in our study because gauges were located upstream of some coastal mountain subcatchments. The Columbia R. had a strongly attenuated hydrograph owing to large watershed size, highly regulated flow, and a warmer-drier climate than other SC watersheds (e.g., 34% vs. >44% PAS respectively). The RC watershed type showed a pluvial streamflow regime owing to warm continental temperatures and rain-dominated precipitation (2%–12% PAS).

3.3. Mean Annual Runoff Across Watershed Types

The average MAR varied dramatically between several watershed types, such as RHN versus RHS, while there was also substantial overlap between other types (e.g., GMM vs. SMC; Table 2, Figure 5a). The association of average MAR with watershed types offered a means to characterize broad spatial patterns of observed MAR

Table 2
Summary Statistics for Mean Annual Runoff (MAR) and Dissolved Organic Carbon (DOC), Calculated Across All Watersheds With Data, in Each of the 14 Watershed Types Draining to the Northeast Pacific Coastal Temperate Rainforest of North America (NPCTR) Margin

Watershed type	MAR (mm)	MAR range (mm)	MAR (n)	DOC (mg L^{-1})	DOC range (mg L^{-1})	DOC (n)
GMH	4,954 (NA)	NA	1	0.99 (0.55)	0.60–1.38	2
GMM	2,325 (738)	1,498–3,894	10	1.08 (0.33)	0.60–1.73	13
SMX	2,691 (1,182)	1,562–4,009	4	1.81 (0.32)	1.58–2.04	2
SMN	4,226 (NA)	NA	1	NA (NA)	NA-NA	NA
SMC	2,101 (798)	813–3,806	22	1.94 (1.05)	0.87–4.63	11
RMN	2,396 (537)	1,714–3,315	6	4.48 (3.51)	1.12–8.40	4
RHN	2,741 (838)	1,962–3,627	3	7.54 (2.63)	3.75–12.49	7
RLN	NA (NA)	NA-NA	NA	6.28 (4.36)	2.76–11.16	3
RMC	3,910 (1,750)	1,137–6,849	8	3.36 (2.20)	0.78–8.10	11
RHC	1,562 (601)	735–2,623	20	2.03 (1.05)	0.91–4.69	11
RLC	694 (291)	262–1,034	8	3.12 (1.90)	1.56–5.42	5
RHS	1,298 (699)	572–2,873	11	1.34 (0.51)	0.57–2.17	13
SC	747 (364)	305–1,324	6	2.16 (0.96)	1.25–3.49	5
RC	620 (176)	480–854	4	1.54 (0.18)	1.39–1.74	3

Note. The standard deviation is reported in brackets. The sample size (*n*) represents the number of watersheds with field observations.

across the region. However, a few types were poorly constrained, with only one to a few gauges or high variability among gauges (e.g., GMH, SMX, SMN, and RHN).

Among coastal watersheds, the GMH (*n* = 1) type had the highest runoff (4,954 mm; Table 2, Figure 5a). This was more than double the mean MAR of the GMM type (2,325 ± 738 mm), which had much lower ice cover and much lower precipitation, partly because some GMM watersheds extended into the lee of the coastal mountains. Mean MAR was also *very high* (>3,500 mm) in the SMN and RMC watershed types, where glaciers were absent or very small, but MAP was very high (Table 1). *High* mean MAR values (2,000–3,000 mm) were observed in the remaining northern watershed types (SMX, RHN, and RMN) as well as the snow mountains of the central zone (SMC), all of which received high MAP. Rain hills of the central and southern zones (RHC, RHS) had *moderate* runoff (1,000–2,000 mm mean MAR), reflecting a drier climate toward the south and in the rain-shadow of coastal mountain ranges. Mean MAR from either continental watershed type (SC: 747 ± 364 mm, RC: 620 ± 176) was much lower than any of the coastal watershed types (Figure S7 in Supporting Information S1), except the rain (shadow) lowland watershed of the central zone (RLC) with 694 ± 291 mm, which clearly reflected the low rates of precipitation inputs to these three watershed types (Table 1, Figure S8 in Supporting Information S1). Long residence times in the (large) continental watersheds likely contributed to low runoff ratios (Figure S8 in Supporting Information S1).

Much of the watershed-level variation in MAR was associated with gradients of precipitation (water inputs), glacier cover (negative mass balance), evapotranspiration rate, and watershed size (water losses; Figure 5b, Figure S8 in Supporting Information S1). Some of the variation may be due to human alteration of watersheds. For example, very low runoff ratios (MAR:MAP) in the rather wet Skokomish (2,996 mm MAP, RMC) and Sawmill Creek (4,220 mm MAP, SMX) watersheds were likely caused by the dams and diversions present in those watersheds.

3.4. Seasonality of Riverine DOC Concentration Across Watershed Types

Like streamflow regimes, broad patterns of DOC seasonality also appeared to be associated with watershed type (Figure 6), although the available data were too sparse to recognize or reject the possibility of distinct DOC seasonality for each type. Most of the watershed types had elevated average DOC concentrations in October or
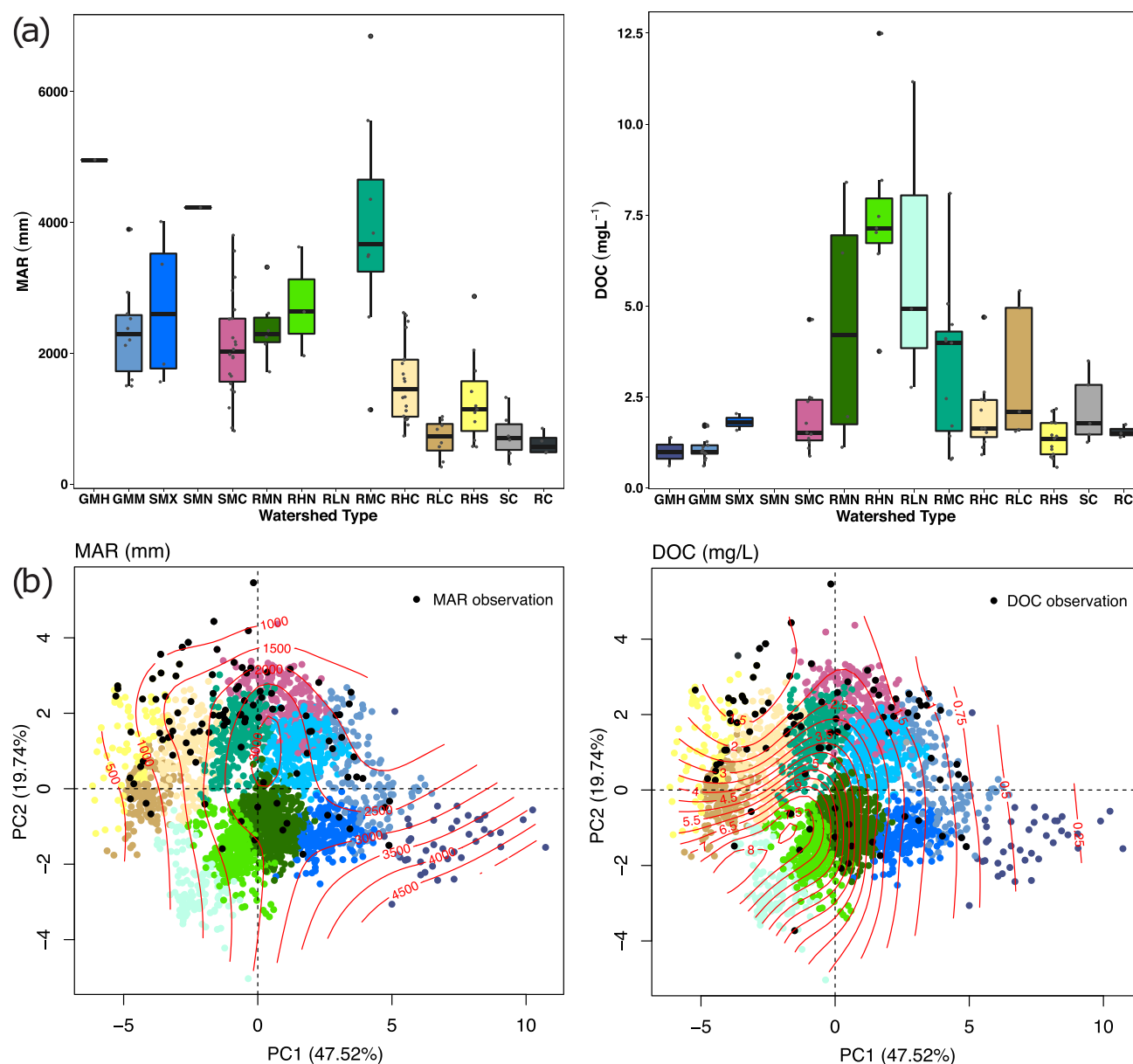
Figure 5. Variation of river Mean Annual Runoff (MAR) (*n* = 104) and mean dissolved organic carbon (DOC) (*n* = 90) concentration across watershed types (a) and across all watershed polygons (b). In (a), the distribution of observed values is show by boxplots and individual watershed values are shown as small gray dots. In (b), black dots represent watersheds with riverine MAR and DOC observations, on a plot of PC1 versus PC2 (Figure 2). Colors indicate the watershed type for watersheds without observations. Contour lines represent predicted mean values from generalized additive models using PC1 and PC2 as interacting predictors. For MAR, repeat (10 times) 10-fold cross-validation indicates adjusted $R^2 = 0.321 \pm 0.026$ SD and mean deviance explained = $52.34 \pm 2.61\%$ SD. For DOC, cross-validation indicates adjusted $R^2 = 0.694 \pm 0.028$ SD and mean deviance explained = $77.24 \pm 1.78\%$ SD.

November, presumably associated with flushing of vegetation and soil organic matter during fall rains. This was observed across a wide range of watershed characteristics and geographic locations, from the RHS of California to the GMH of Southeast Alaska. In two of the northern rain types (RHN and RMN), DOC tended to begin increasing in summer—earlier than DOC increased in the rain types further south (e.g., RHC and RLC). The apparent August peak in RHN and RMN (Figure 6) may be an artifact of missing August data at some lower-DOC watersheds (see Giesbrecht et al., 2022 data package). However, a few data rich watersheds in RHN confirmed a DOC increase starting in mid-summer, followed by maximum mean concentrations in September/October.
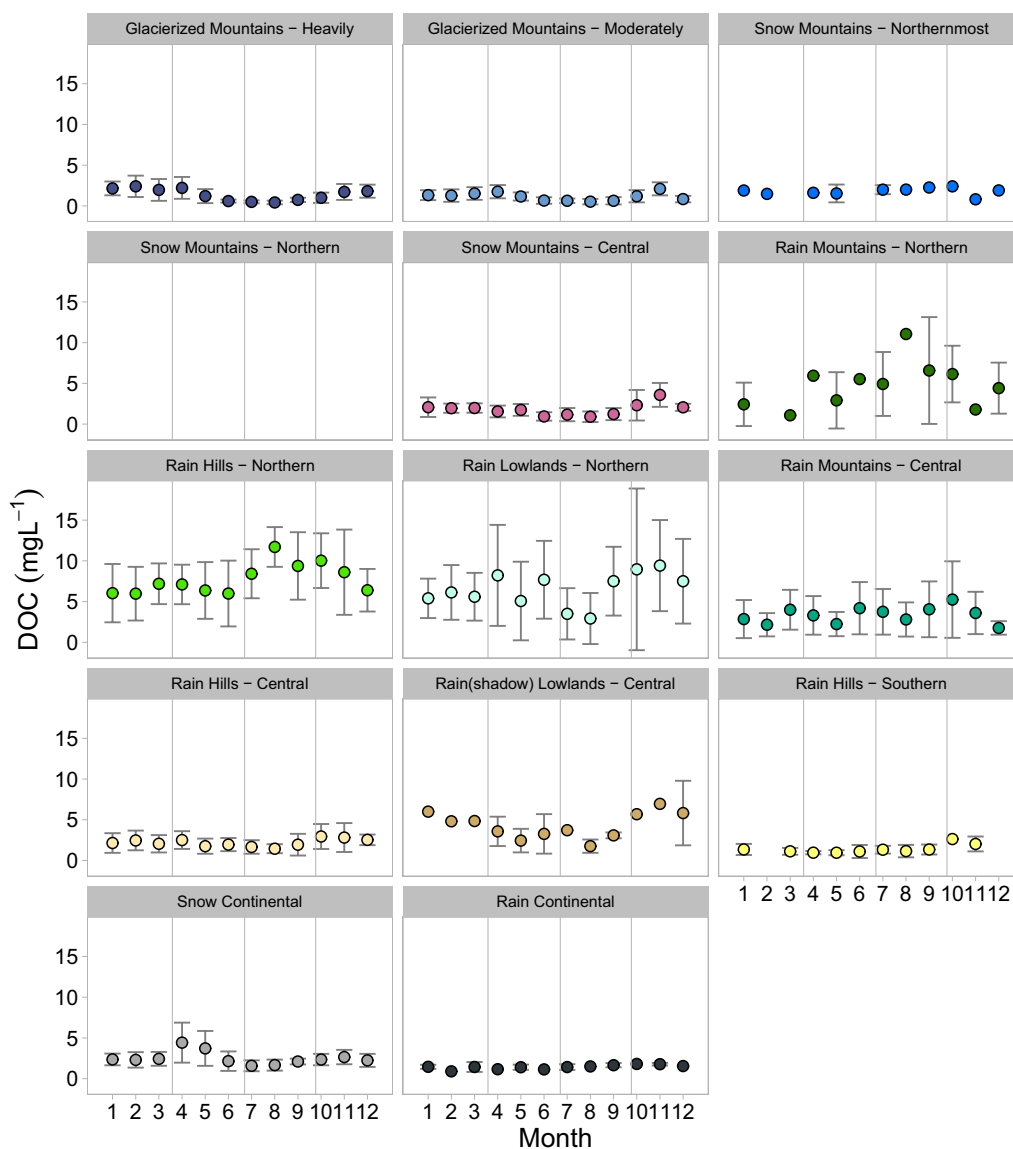
Figure 6. Observed dissolved organic carbon (DOC) regimes by watershed type, for all $n = 90$ watersheds with DOC observations. Dots represent the average of mean monthly DOC concentrations observed across watersheds, for a given cluster. The number of sampled watersheds varies from 2 to 13 (see Figure 5). Error bars represent the standard deviation across watersheds (spatial variation). Vertical reference lines mark the divisions between the four astronomical seasons: winter, spring, summer, and fall.

The SC type was unique in having a distinct and dominant spring DOC peak (>4 mg L^{-1}) just as streamflow increased due to snowmelt. This constituted an approximate doubling of DOC concentration in April compared to the preceding winter months. The GMM type showed a subtle increase in DOC in spring on average (Figure 6). No DOC data were available for the SMN type. Both glacierized watershed types (GMH and GMM) were characterized by a strong dilution effect during the meltwater season. In summary, the 14 watershed types appeared to capture four general patterns of DOC seasonality, which can be named by the dominant process: *spring flushing*, *summer diluting*, *summer-fall flushing*, and *fall flushing*.

Table 3
Importance of Each Watershed Type in Terms of Proportion of Total Regional Area, Precipitation (Rain and Snow), Precipitation as Snow (in Snow Water Equivalent), and Glacial Ice Cover

Watershed type	Area		Precipitation		Precipitation as snow		Glacial ice	
	Area (km^2)	% of region	Volume (km^3)	% of region	Volume (km^3)	% of region	Area (km^2)	% of region
GMH	15,738	1.1	70.2	3.8	44.4	7.2	10,068.7	30.7
GMM	58,189	4.0	158.5	8.5	83.3	13.5	9,457.2	28.8
SMX	10,703	0.7	44.0	2.4	13.3	2.2	184.7	0.6
SMN	18,329	1.3	81.5	4.4	21.1	3.4	41.4	0.1
SMC	68,958	4.8	154.7	8.3	45.9	7.4	1,630.0	5.0
RMN	25,691	1.8	81.3	4.4	14.8	2.4	1.5	<0.1
RHN	16,463	1.1	45.8	2.4	4.8	0.8	0.0	0.0
RLN	6,403	0.4	14.3	0.8	0.9	0.2	0.0	0.0
RMC	24,957	1.7	91.9	4.9	10.0	1.6	34.8	0.1
RHC	35,547	2.5	79.6	4.3	5.0	0.8	0.0	0.0
RLC	10,072	0.7	13.9	0.7	0.4	0.1	0.0	0.0
RHS	26,717	1.9	48.9	2.6	0.8	0.1	0.0	0.0
SC	1,049,604	72.7	892.8	47.8	365.3	59.2	11,421.2	34.8
RC	75,690	5.2	90.6	4.9	6.9	1.1	2.3	<0.1
Coastal (SCR) total	317,768	22	884	47	245	40	21,418	65.2
Regional total	1,443,062	100	1,868	100	617	100	32,842	100.0

3.5. DOC Concentration Across Watershed Types

As we hypothesized, mean and median DOC at river outlets varied with watershed type (Table 2, Figure 5a). Mean DOC was *high* (>4 mg L^{-1}) in northern rain types (RMN, RHN, and RLN), *moderate* (3–4 mg L^{-1}) in RLC and RMC, and *low* (<2.5 mg L^{-1}) in the remaining watershed types. The lowest mean DOC was observed in the two glacierized mountain watershed types (GMH and GMM). Notably, the SC watershed type had higher mean DOC than several coastal watershed types (Table 2), which was due to higher concentrations in the Fraser (3.49 ± 1.76 mg L^{-1}, $n = 470$) and Skeena (2.83 ± 1.89 mg L^{-1}, $n = 461$) rivers (Figure S7 in Supporting Information S1).

The defining characteristics of the watershed types appear to impose broad scale spatial controls on DOC concentration. Slope alone was only weakly correlated with DOC concentration, over such a wide range of climatic conditions (Figure S9 in Supporting Information S1). Rather, the three watershed types with high DOC (RMN, RHN, and RLN) were characterized by terrain with comparatively low to moderate slope and elevation and a perhumid coastal climate with comparatively low evapotranspiration and high precipitation (Figure 5b). The sampled southern rain hill (RHS) watersheds were not consistently steeper than the rain hills and mountains of the north (RHN, RMN), yet stream DOC concentrations were low (Figure S9 in Supporting Information S1), suggesting the southern climate limited DOC concentrations in streams.

3.6. Regional-Scale Importance of Contrasting Watershed Types

Summed over the regional scale, watershed types had different total areal extents, total magnitude of water inputs, and total glacier cover. We found that the 10 continental watersheds dominated the total regional area (78% of area), yet captured only 53% of total precipitation due to lower rates of precipitation per unit area (Table 3). By contrast, the SCR watersheds were disproportionately effective at capturing precipitation (47% of regional total), snow (40%), and glacial cover (65%), despite occupying only 22% of the regional area.

Three of the SCR watershed types stood out for making an individually large contribution to total regional precipitation-capture and ice-storage. The GMM and SMC watershed types captured the greatest percentages

of total regional precipitation volume (8.5% and 8.3%, respectively) and total precipitation as snow (13.5% and 7.4%), among SCR watersheds. The GMH and GMM watershed types each held more than a quarter of regional ice cover (30.7% and 28.8%), while the SMC type held another 5.0% (Table 3). Individual rain types ranked low in terms of regional importance, because of a more finely divided classification, yet the seven coastal rain types when combined captured more of the total regional area (10.1%) and precipitation (20.1%) than either the combined glacierized types (5.1% of area and 12.2% of precipitation) or the combined snow types (6.8% of area and 15.0% of precipitation).

4. Discussion

4.1. A Conceptual Model of Hydro-Biogeochemical Watershed Types

In this study, we found that the statistical clustering of watersheds into coherent watershed types provided an effective framework for describing the complex spatial gradients of catchment characteristics, streamflow regimes, and DOC concentrations across SCR watersheds of the NPCTR margin. Based on these findings, we developed a conceptual model of the 14 watershed types and their distinguishing characteristics (Figure 7). The mechanistically supported links between watershed type and river hydro-biogeochemistry (Figure 7) allow us to extrapolate broad spatial patterns (Figure 3) of typical river conditions across the extensive ungauged and unsampled areas in this region, while recognizing that individual watersheds will vary from these typical conditions at a local scale. Similar approaches may be informative in other complex regions globally, particularly those with sparse field observations.

4.2. Dominant Streamflow Patterns and Hydro-Biogeochemistry

A map of typical streamflow seasonality should serve as a solid foundation for thinking about hydrologic controls on biogeochemical cycling across a region. Our findings corroborate previous characterizations of streamflow patterns at the land-sea interface in the NPCTR and allow for the first regionally unified synthesis. Glacial and glacier supported regimes (Figure 7) are limited to high mountain watersheds in Southeast AK and BC (Figure 3), while a topographically controlled mix of pluvial and rain-snow hybrid regimes dominate the rest of the SCR watersheds of Southeast AK (Curran & Biles, 2021; Edwards et al., 2013; O'Neel et al., 2015; Sergeant et al., 2020), BC (Bidlack et al., 2021; Eaton & Moore, 2010; Trubilowicz et al., 2013; Wade et al., 2001), and WA from Puget Sound northward (Fleming et al., 2007; Reidy Liermann et al., 2012; Sanborn & Bledsoe, 2006). Pluvial-dominated hydrographs are nearly ubiquitous among SCRs south of Puget Sound WA (Bidlack et al., 2021; Lane et al., 2018; Reidy Liermann et al., 2012; Sanborn & Bledsoe, 2006), with a distinct "dry season" in CA (McManamay et al., 2014; Roden, 1967). By contrast, the comparatively "pure" nival regimes (Figure 7) are limited to the few large continental rivers that penetrate the coastal mountains from colder climates; for example, Skeena R. (Morrison et al., 2012) and Fraser R. (Fleming et al., 2007; Figure 3). Importantly, these long-term average streamflow regime descriptions do not account for interannual climatic variations such as La Niña years, which can introduce a small snowmelt freshet to otherwise pluvial watersheds including our RHC type (Fleming et al., 2007).

Our study builds on previous work by highlighting the diversity of glacial, pluvial, and hybrid streamflow regime types along this broad coastline, which may have ecosystem-level implications. Glacial types vary from a highly glacial-dominated regime (GMH; e.g., Sergeant et al., 2020) to a glacier supported nival regime (GMM), while a three-way hybrid regime (*nival-glacial-pluvial*; Eaton & Moore, 2010; Trubilowicz et al., 2013) is found in a subset of GMM watersheds (Giesbrecht et al., 2022). Across these systems, the relative contribution of icemelt, snowmelt, and rainwater sources is expected to correspond with contrasting organic matter sources in streams (Hood et al., 2009; Fellman et al., 2014) and to impact the timing and quality of carbon subsidies to the coastal ocean (Arimitsu et al., 2018; St. Pierre et al., 2020). Among the non-glacierized watershed types, low-flow duration, magnitude, and timing varies dramatically across the region (Figure 7), which may have a number of implications for aquatic ecosystems, including shifts between allochthonous and autochthonous dominated energy sources (Rolls et al., 2012) and the survival of anadromous fish (Atlas et al., 2021; Obedzinski et al., 2018; Sergeant et al., 2017).
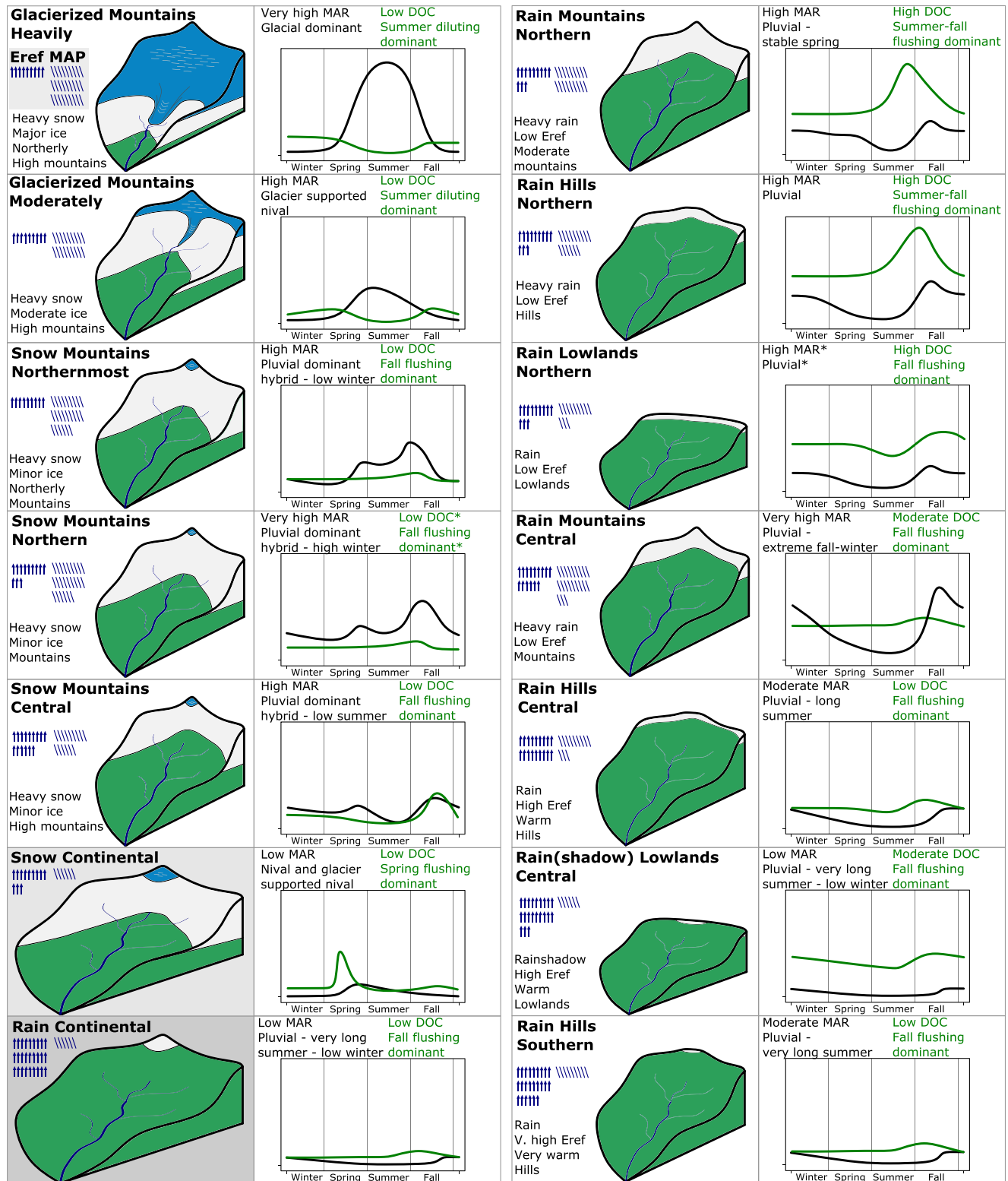
Figure 7.

4.3. Rainforest Runoff to the Ocean in Global Context

Earth's coastal temperate rainforest margins are thought to play an important role in linking the biogeochemical cycles of terrestrial and marine systems due to high yields of freshwater (Bidlack et al., 2021). In the global context, all but one of the NPCTR coastal watershed types are (on average) considered *wet rivers* (>750 mm yr^{-1})—the wettest of a four-category classification by Milliman and Farnsworth (2011). Even the two continental watershed types and the coastal rainshadow type (RLC) rank as *humid rivers* (250–750 mm yr^{-1})—the second wettest group of rivers globally. Other regions with a high proportion of wet coastal rivers include temperate mountains of Chile and New Zealand, and tropical mountains of Central America, the Amazon basin, Asia and Oceania (Milliman & Farnsworth, 2011). A number of studies have reported particularly high runoff rates in the SCR zone of southeast Alaska (e.g., Beamer et al., 2017; Edwards et al., 2021; Neal et al., 2010; J. Wang et al., 2004) and BC (Morrison et al., 2012), which is driven by combinations of high precipitation inputs, low evapotranspiration (T. Wang et al., 2016), and high rates of glacial mass loss (Beamer et al., 2017; Clarke et al., 2015). By contrast, the drier and ice-free coastal watersheds of Oregon and California have much lower runoff (Figure 5a). Our results highlight the degree of local-scale and regional-scale spatial variability in MAR within the NPCTR region, which is mechanistically linked to watershed characteristics and broadly represented by our classification system (Figure 7).

4.4. Freshwater DOC Hot Spots and Hot Moments

In our conceptual model (Figure 7), each of the watershed types has an associated (in some cases unique) combination of mean DOC concentration and DOC seasonality. For example, RMN and RHN have high mean DOC and a summer-fall flushing regime, while GMH and GMM have low DOC and a summer diluting regime. These hydro-biogeochemical associations suggest that our classification of watershed types (Figure 3) can be used to map DOC patterns (Figure 7) across this large, hydrologically diverse region. Regional maps of biogeochemical hot spots and hot moments (McClain et al., 2003) can potentially be applied in research (e.g., cross-ecosystem resource subsidies; Bidlack et al., 2021) and environmental management (e.g., greenhouse gas emissions, downstream hypoxia, drinking water treatment, and pollutant transport; McClain et al., 2003).

Maps of field-validated watershed types can be used to infer spatial controls on the distribution of DOC hotspots and coldspots. The hotspot watershed types (RHN, RLN, and RMN) of the NPCTR margin are found where comparably low topographic relief coincides with a hypermaritime climate (high precipitation, relatively low evapotranspiration, and ocean-moderated temperatures), promoting accumulation of soil organic matter (Banner et al., 1983; McNicol et al., 2019) and DOC export from both wetland and hillslope sites (Banner et al., 2005; D'Amore et al., 2016; Fellman et al., 2009; Gibson et al., 2000; Oliver et al., 2017). By contrast, DOC coldspots are associated with a broad range of source-limiting factors, including extensive glacial ice and steep mountainous terrain with low soil organic carbon (SOC; e.g., Hood & Berner, 2009), continental climates, large catchments, or warm coastal climates with high evapotranspiration (e.g., Butman et al., 2016). Understanding the impact of climate change on DOC export will be challenging without knowledge of such catchment-specific controlling mechanisms.

Mapping hydro-biogeochemical watershed types also helps to reveal the spatial extent of different climatic and hydrological controls on DOC concentration dynamics. Some degree of fall-flushing of DOC from vegetation and soils by rain appears to occur across the majority of this region, from small bog-forest and glacierized catchments of southeast Alaska (Fellman et al., 2014), to the large continental Fraser River (Voss et al., 2015), to warmer catchments of Oregon (Hood et al., 2006) and California (Oliver et al., 2016). In the DOC concentration hotspots of the perhumid rainforest (i.e., RHN and RMN), DOC tends to increase earlier (in summer), which has

Figure 7. Conceptual model of 14 watershed types draining to the NPCTR margin, with illustrations of typical streamflow regimes (specific discharge) and dissolved organic carbon (DOC) seasonality (concentration). Within each type, graphical elements indicate the relative ranking of the watershed type in terms of topography (mountains, hills, lowlands), snow inputs, glacier cover, evapotranspiration (small upwards blue arrows), and total precipitation (small blue slashes). Corresponding text fields describe key watershed characteristics and provide a classification of MAR, streamflow patterns, mean DOC concentration, and dominant patterns of DOC seasonality. Each of the watershed types has a distinct combination of these hydro-biogeochemical categories, providing a simple conceptual model for characterizing and mapping the region. For example, SMX watersheds typically have a pluvial dominant hybrid streamflow regime that is low in winter ("low winter") whereas SMN watersheds typically have a pluvial dominant hybrid regime distinguished by higher flows in winter ("high winter"). * indicates where data were unavailable, yet the hydro-biogeochemical regime was inferred from watershed characteristics. MAR grouping thresholds: low, <1,000 mm; moderate, 1,000–2,000 mm; high, 2,000–3,000 mm; very high, >3,000 mm. DOC grouping thresholds: low, <2.5 mg L^{-1}, moderate, 3–4 mg L^{-1}, high >4 mg L^{-1}.

been linked to rain occurring after a period of warm dry weather (D'Amore et al., 2015; Fellman et al., 2014; Oliver et al., 2017; St. Pierre et al., 2020). While rain-induced flushing processes are dominant in non-glacierized SCR watersheds, glacierized watershed types are characterized by strong declines in DOC concentration during the summer months when specific discharge is high – a meltwater dilution process previously observed in northern southeast Alaska (Fellman et al., 2014; Hood & Berner, 2009) and now as far south as Bute Inlet on the BC coast. Spring-flushing of DOC to rivers can occur when the initial snowmelt creates shallower flowpaths and greater hydrologic connectivity to source pools during early freshet (e.g., Fraser River; Voss et al., 2015). In our assessment of the NPCTR coastline, this process was only clearly dominant in the SC watershed type (Figure 7), with a subtler influence in glacierized watersheds, indicating that rain—in combination with seasonal temperature—exerts the dominant control on DOC flushing in the non-glacierized watersheds of the SCR zone (Figure 7).

This regional synthesis of spatial controls on DOC patterns should be considered a first approximation that requires further refinement with better observational data coverage in both spatial and temporal dimensions. Field observations remain sparse in the hotspot watershed types of BC and AK (Figure S7 in Supporting Information S1), which span a range of watershed properties (Figure 5b). High frequency measurements in key watershed types could better resolve rapid DOC dynamics during early freshet (Voss et al., 2015) as well as summer and fall rain events (Fellman et al., 2009). Direct assessment of concentration-discharge relationships across the diverse watershed types of this region could help tease apart the relative contributions of flow, temperature, and meltwater timing to DOC dynamics more generally (e.g., Gómez-Gener et al., 2021; Winterdahl et al., 2014; Zarnetske et al., 2018). Furthermore, data from this region could be used to determine if DOC export is source limited across the extensive glacierized watershed types (e.g., Hood et al., 2020) in contrast to the more general pattern of transport limited DOC export from non-glacierized watershed types (Hood et al., 2020; Zarnetske et al., 2018).

4.5. Implications for Understanding the Impacts of Climate Change

Climate change is likely altering the spatial mosaic of watershed types and the corresponding hydro-biogeochemical regimes of rivers in this region. The general direction of change can be hypothesized by making space-for-time substitutions in Figure 2 (supported by Figure 5b and Figure S3 in Supporting Information S1), with limitations. In our ordination biplot, there is a strong spatial gradient from cold watersheds in the right/lower-right to warm watersheds in the left/upper-left. Consequently, we predict a temporal shift along this thermal gradient as the climate changes to higher MAT and Eref and lower PAS (T. Wang et al., 2016) and glacier cover (Clarke et al., 2015). Based on this, we hypothesize that the extensive snow mountain watersheds (97,990 km^2) will develop streamflow and DOC regimes more like current rain mountain watersheds with similar topography (see Figure 7). Similarly, glacierized mountain watersheds are likely to become more like current snow mountain watersheds of similar size and topography. For example, higher winter flows, lower summer flows, and less dilution of DOC during the summer. This could cause a shift from source limited to transport limited DOC flux (Hood et al., 2020) over the large area of moderately and heavily glacierized watersheds (73,927 km^2). These hydro-biogeochemical changes can be expected to lag behind climate change due to the time needed for glacial mass loss and the development of soil and forest biomass. Furthermore, long-term watershed adjustments may be complicated by anthropogenic disturbance (e.g., Wolf et al., 1995) and by legacy glacial sediments that influence river biogeochemistry (Anderson, 2007; Church & Slaymaker, 1989).

The future of rain watershed types is more difficult to predict with a space-for-time substitution. We expect the MAT and Eref of northern rain watersheds to increase (T. Wang et al., 2016) and become more like the central rain watersheds (i.e., a shift to the upper left in Figure 2), leading to reduced snowmelt influence on streamflow, for example (Bidlack et al., 2021). However, climate change may also increase MAP over time within the northern and central part of this region (Shanley et al., 2015; T. Wang et al., 2016). As a result, the (already drier) RHC and RLC watersheds are not good substitutes for the future streamflow magnitude of the (already wetter) RHN and RLN watersheds. Changing seasonality of rainfall (e.g., less in summer and more in fall; Schnorbus et al., 2014) and increasing frequency of extreme atmospheric river events (Radić et al., 2015) must also be considered, in a spatially explicit framework. Future DOC regimes may also depend on the uncertain fate of existing SOC stocks (Fellman et al., 2017), which are currently higher in the northern rain watersheds than in the warmer central group

(McNicol et al., 2019). Finally, watersheds at the southern margin (RHS) have no spatial analogue in our study area because they already occupy the thermal extreme of this region.

A quantitative analysis of projected watershed-climates and river hydro-biogeochemistry is clearly warranted, with consideration of both long-term averages and extreme events. In such an analysis, we might expect the emergence of no-analogue hydro-biogeochemical watershed types owing to novel combinations of climate, glaciers, and topography, warmer temperatures than historically observed for any watersheds in the region, legacy sediments and soil carbon, time-lags in ecosystem development, and human alteration of watersheds. In the meantime, our spatially explicit classification map can be used—in combination with existing projections and process-knowledge—to hypothesize how climate change will continue to play out across the mosaic of watershed types in this region. The expected changes have implications for both runoff (Beamer et al., 2017; Bidlack et al., 2021; Crumley et al., 2019; Curry et al., 2019; Littell et al., 2018; Moore et al., 2009; Radić et al., 2015; Reidy Liermann et al., 2012; Rolls et al., 2012; Schnorbus et al., 2014; Shanley et al., 2015; Stahl & Moore, 2006) and organic carbon (Bidlack et al., 2021; Edwards et al., 2013; Fellman et al., 2017; Hood & Berner, 2009; Hood et al., 2020; Milner et al., 2017).

4.6. Hydro-Biogeochemical Mapping and Modeling in Poorly Sampled Regions

Watershed classification maps have many potential applications for understanding biogeochemical patterns and processes at local, regional, and global scales. While we used DOC for our case study, we hypothesize that other biogeochemical components and properties may also vary with watershed types defined by climate, glaciers, topography, and vegetation. In particular, dissolved organic nitrogen and iron are transported in association with DOC in DOM (Kritzberg et al., 2014; Schroth et al., 2011; St. Pierre et al., 2021; Sugai & Burrell, 1984) and should also vary with these watershed types. Stream temperature is strongly influenced by climate, topography, and glacier cover and further modified by residence time (Fellman et al., 2014; Hood & Berner, 2009; Winfree et al., 2018) and riparian vegetation. Glacierized watershed types are likely to have distinct biogeochemical signatures because glacial activity accelerates physical and chemical weathering of rock, potentially enhancing the supply of total suspended sediments, phosphorous (Hodson et al., 2004; Hood & Berner, 2009), petrogenic particulate organic carbon (Hood et al., 2020), and dissolved inorganic carbon (DIC; Tank et al., 2012). These watershed types may also reflect the effect of topographic relief on landscape denudation rates and thus river sediment loads (Milliman & Syvitski, 1992).

Topo-climatic focused watershed types would not be expected to represent the effect of lithology (e.g., carbonate vs. acid plutonic rock) on the supply of constituents such as dissolved silica (e.g., Jansen et al., 2010), calcium (e.g., Mosher et al., 2010), or DIC (Tank et al., 2012). However, they should capture the broad effect of climate on chemical weathering rates (Phillips & Cowling, 2019; Schlesinger, 1997) and the effect of runoff on flowpath and dilution (Schlesinger, 1997). Importantly, agricultural, urban, and atmospheric pollution were not considered here and could be key determinants of constituents such as nitrogen (Bouwman et al., 2009; Mayorga et al., 2010), particularly in the southern and central NPCTR where watersheds have more human population, industry, and agriculture (Wolf et al., 1995). Human-alteration of watersheds may also play a changing role in determining spatial patterns of streamflow and DOC dynamics (e.g., Lajtha & Jones, 2018). More broadly, a range of other watershed characteristics and associated processes (e.g., cycling in lakes and stream networks, forest management, and forest fire) may be important for understanding biogeochemical cycling of carbon and other elements.

We can imagine many extensions—or alternatives—to this classification. Any classification is sensitive to the defining goals, variables, analytical methods, and other procedural decisions (Figure 1; e.g., Melles et al., 2014; Olden et al., 2012; Soranno et al., 2010). For example, streamflow regimes alone might be mapped more precisely by training predictive models to estimate catchment-level hydrographs as a function of individual watershed characteristics (e.g., Trubilowicz et al., 2013). Inter-annual variability in stream hydro-biogeochemical regimes could be characterized and related to climatic variation for each watershed type (e.g., Eaton & Moore, 2010; Fleming et al., 2007). Future work could also attempt to subdivide our (or other) watershed types based on additional controlling factors such as geology, lakes, water regulation, urbanization, or land management (see nested hierarchical approaches such as the REC system; Snelder & Biggs, 2002). This should lead to watershed types with less internal variation in stream hydro-biogeochemistry. However, further splitting would also lead to fewer independent validation sites per watershed type and may contribute to the problem of unvalidated classification

systems (Melles et al., 2014). Where data are available, watershed classification offers a potentially powerful tool to stratify complex regions and evaluate specific hypotheses about anthropogenic effects within types (e.g., Snelder & Biggs, 2002).

5. Conclusions

To our knowledge, this is the first study to assess streamflow regimes with an exhaustive empirical data set spanning the full NPCTR margin and the first to validate a regional watershed classification with field observations of both streamflow and carbon dynamics. The resulting map of hydro-biogeochemical watershed types may serve as a spatially explicit framework for thinking about fluvial connections across the land-sea interface. These diverse sources of freshwater runoff are thought to merge and form an oceanographically distinct zone known as the Riverine Coastal Domain (Carmack et al., 2015). The dramatic spatial heterogeneity of discharge and DOC timing and magnitude may have implications for the seasonality of coastal ocean processes and nearshore ecosystems. This is consistent with the idea that small but numerically abundant SCR watersheds (or "small mountainous rivers") make distinct and important line source contributions to land-sea connectivity globally (Goñi et al., 2013; Lyons et al., 2002; Milliman & Syvitski, 1992; Royer, 1982; Wheatcroft et al., 2010). Climate change is acting rapidly in this region, with consequences that vary by watershed type, potentially creating no-analogue conditions along the land-ocean aquatic continuum. A key challenge for coastal margin scientists and managers is to understand how these interacting and changing spatial gradients in the freshwater realm shape the seasonal cycles, physical structure, and carbon dynamics of the coastal ocean now and in the future.

While watershed classification methods are diverse and well developed in hydrology (e.g., Olden et al., 2012), comparatively little has previously been done to integrate both streamflow and biogeochemistry in regional watershed classification. A wide range of classification approaches could be explored and broad frameworks have emerged in the context of conservation planning and ecosystem management (Melles et al., 2014; Ouellet Dallaire et al., 2019; Snelder & Biggs, 2002; Soranno et al., 2010; Wolock et al., 2004). An advantage of the approach developed here is that the classification itself was based on globally available geospatial data products and was subsequently validated with available field observations from a wide range of watershed types. This approach may be applicable in other data poor and transboundary regions. However, a shortage of spatially and temporally representative field data may be the key constraint on hydro-biogeochemical classification and spatial modeling (see also Li et al., 2021). Substantial funding and international coordination efforts are needed to collect (McClelland et al., 2015) and synthesize (Bidlack et al., 2017) long-term and consistent river observations across national borders. Watershed-based classification can inform the design of optimized river observation networks (Wolock et al., 2004). Watershed-informed observation networks may, in turn, prove useful for ecosystem-based management and conservation planning, because watersheds "represent, without having to undertake a significant data gathering and planning exercise, a "complete" sample of ecosystems and communities from headwaters to tidewater" (Lertzman & MacKinnon, 2013, p. 224). Furthermore, we suggest that watershed classification could be used to stratify the spatial heterogeneity that currently hinders development of integrated hydro-biogeochemical theories (Li et al., 2021). Given the breadth of potential applications, we encourage further development of representative datasets and methodological frameworks for hydro-biogeochemical watershed classification.

Data Availability Statement

The datasets for this research are available as an open access data package on DRYAD (Giesbrecht et al., 2022; license CCO 1.0 Universal [CCO 1.0]), including created data and compiled (processed) data. The source data sets are cited in the manuscript and in the data package.

References

Aitkenhead-Peterson, J. A., Alexander, J. E., & Clair, T. A. (2005). Dissolved organic carbon and dissolved organic nitrogen export from forested watersheds in Nova Scotia: Identifying controlling factors. *Global Biogeochemical Cycles*, 19(4), 1–8. https://doi.org/10.1029/2004gb002438

Alaback, P. B. (1996). Biodiversity patterns in relation to climate: The coastal temperate rainforests of North America. In R. G. Lawford, E. Fuentes, & P. B. Alaback (Eds.), *High-latitude rainforests and associated ecosystems of the west coast of the Americas: Climate, hydrology, ecology, and conservation* (pp. 105–133). Springer. https://doi.org/10.1007/978-1-4612-3970-3_7

Anderson, S. P. (2007). Biogeochemistry of glacial landscape systems. *Annual Review of Earth and Planetary Sciences*, 35, 375–399. https://doi.org/10.1146/annurev.earth.35.031306.140033

Arimitsu, M. L., Hobson, K. A., Webber, D. N., Piatt, J. F., Hood, E. W., & Fellman, J. B. (2018). Tracing biogeochemical subsidies from glacier runoff into Alaska's coastal marine food webs. *Global Change Biology*, *24*(1), 387–398. https://doi.org/10.1111/gcb.13875

Atlas, W. I., Seitz, K. M., Jorgenson, J. W. N., Millard-Martin, B., Housty, W. G., Ramos-Espinoza, D., et al. (2021). Thermal sensitivity and flow-mediated migratory delays drive climate risk for coastal sockeye salmon. *Facets*, *6*(1), 71–89. https://doi.org/10.1139/facets-2020-0027

Banner, A., LePage, P., Moran, J., & de Groot, A. (2005). *The HyP3 Project: Pattern, process, and productivity in hypermaritime forests of coastal British Columbia: A synthesis of 7-year results*. Retrieved from http://www.for.gov.bc.ca/hfd/pubs/docs/srs/Srs10.pdf

Banner, A., Pojar, J., & Rouse, G. E. (1983). Postglacial paleoecology and successional relationships of a bog woodland near Prince Rupert, British Columbia. *Canadian Journal of Forest Research*, *13*, 938–947. https://doi.org/10.1139/x83-125

Bauer, J. E., Cai, W.-J., Raymond, P. A., Bianchi, T. S., Hopkinson, C. S., & Regnier, P. A. G. (2013). The changing carbon cycle of the coastal ocean. *Nature*, *504*, 61–70. https://doi.org/10.1038/nature12857

Beamer, J. P., Hill, D. F., McGrath, D., Arendt, A., & Kienholz, C. (2017). Hydrologic impacts of changes in climate and glacier extent in the Gulf of Alaska watershed. *Water Resources Research*, *53*(9), 7502–7520. https://doi.org/10.1002/2016wr020033

Beck, H. E., Zimmermann, N. E., McVicar, T. R., Vergopolan, N., Berg, A., & Wood, E. F. (2018). Present and future Köppen-Geiger climate classification maps at 1-km resolution. *Scientific Data*, *5*, 1–12. https://doi.org/10.1038/sdata.2018.214

Bidlack, A., Bisbing, S., Buma, B., Diefenderfer, H., Fellman, J., Floyd, W., et al. (2021). Climate-mediated changes to linked terrestrial and marine ecosystems across the Northeast Pacific coastal temperate rainforest margin. *BioScience*, *71*(6), 581–595. https://doi.org/10.1093/biosci/biaa171

Bidlack, A., Buma, B., & Butman, D. (2017). *Quantifying Coastal Rain Forest Carbon Transport* (Vol. 98). Eos. https://doi.org/10.1029/2017EO077633

Borja, A., Andersen, J. H., Arvanitidis, C. D., Basset, A., Buhl-Mortensen, L., Carvalho, S., & Teixeira, H. (2020). Past and future grand challenges in marine ecosystem ecology. *Frontiers in Marine Science*, *7*. https://doi.org/10.3389/fmars.2020.00362

Bouwman, A. F., Beusen, A. H. W., & Billen, G. (2009). Human alteration of the global nitrogen and phosphorus soil balances for the period 1970–2050. *Global Biogeochemical Cycles*, *23*(4). https://doi.org/10.1029/2009gb003576

Breiman, L. (2001). Random forests. *Machine Learning*, *45*, 5–32. https://doi.org/10.1023/a:1010933404324

Butman, D., Stackpoole, S., Stets, E., McDonald, C. P., Clow, D. W., & Striegl, R. G. (2016). Aquatic carbon cycling in the conterminous United States and implications for terrestrial carbon accounting. *Proceedings of the National Academy of Sciences of the United States of America*, *113*(1), 58–63. https://doi.org/10.1073/pnas.1512651112

Carmack, E., Winsor, P., & Williams, W. (2015). The contiguous panarctic riverine coastal Domain: A unifying concept. *Progress in Oceanography*, *139*, 13–23. https://doi.org/10.1016/j.pocean.2015.07.014

Castellarin, A., Claps, P., Troch, P. A., Wagener, T., & Woods, R. (2011). Special issue: Catchment classification and PUB. *Hydrology and Earth System Sciences*, *15–16*.

Church, M., & Ryder, J. M. (2010). Physiography of British Columbia. In R. G. Pike, T. E. Redding, R. D. Moore, R. D Winker, & K. D. Bladon (Eds.), *Compendium of forest hydrology and geomorphology in British Columbia*. Retrieved From www.for.gov.bc.ca/hfd/pubs/Docs/Lmh/Lmh66.htm

Church, M., & Slaymaker, O. (1989). Disequilibrium of Holocene sediment yield in glaciated British Columbia. *Nature*, *337*(6206), 452–454. https://doi.org/10.1038/337452a0

Clarke, G. K. C., Jarosch, A. H., Anslow, F. S., Radić, V., & Menounos, B. (2015). Projected deglaciation of western Canada in the twenty-first century. *Nature Geoscience*, *8*(5), 372–377. https://doi.org/10.1038/ngeo2407

Commission for Environmental Cooperation (2009). *Ecological regions of North America. Vector digital data*. Canada. Retrieved From http://www.cec.org/north-american-environmental-atlas/terrestrial-ecoregions-level-iii/

Covino, T., Golden, H. E., Li, H. Y., & Tang, J. (2018). Aquatic carbon-nutrient dynamics as emergent properties of hydrological, biogeochemical, and ecological interactions: Scientific advances. *Water Resources Research*, *54*(10), 7138–7142. https://doi.org/10.1029/2018wr023588

Crumley, R. L., Hill, D. F., Beamer, J. P., & Holzenthal, E. R. (2019). Seasonal components of freshwater runoff in Glacier Bay, Alaska: Diverse spatial patterns and temporal change. *Cryosphere*, *13*(6), 1597–1619. https://doi.org/10.5194/tc-13-1597-2019

Cuevas, L. A., Tapia, F. J., Iriarte, J. L., González, H. E., Silva, N., & Vargas, C. A. (2019). Interplay between freshwater discharge and oceanic waters modulates phytoplankton size-structure in fjords and channel systems of the Chilean Patagonia. *Progress in Oceanography*, *173*, 103–113. https://doi.org/10.1016/j.pocean.2019.02.012

Curran, J. H., & Biles, F. E. (2021). Identification of seasonal streamflow regimes and streamflow drivers for daily and peak flows in Alaska. *Water Resources Research*, *57*. https://doi.org/10.1029/2020wr028425

Curry, C. L., Islam, S. U., Zwiers, F. W., & Déry, S. J. (2019). Atmospheric rivers increase future flood risk in Western Canada's largest Pacific river. *Geophysical Research Letters*, *46*(3), 1651–1661. https://doi.org/10.1029/2018gl080720

D'Amore, D. V., Edwards, R. T., & Biles, F. E. (2016). Biophysical controls on dissolved organic carbon concentrations of Alaskan coastal temperate rainforest streams. *Aquatic Sciences*, *78*(2), 381–393. https://doi.org/10.1007/s00027-015-0441-4

D'Amore, D. V., Edwards, R. T., Herendeen, P. A., Hood, E., & Fellman, J. B. (2015). Dissolved organic carbon fluxes from hydropedologic units in Alaskan coastal temperate rainforest watersheds. *Soil Science Society of America Journal*, *79*, 378–388. https://doi.org/10.2136/sssaj2014.09.0380

Detenbeck, N. E., Elonen, C. M., Taylor, D. L., Anderson, L. E., Jicha, T. M., & Batterman, S. L. (2003). Effects of hydrogeomorphic region, catchment storage and mature forest on baseflow and snowmelt stream water quality in second-order Lake Superior Basin tributaries. *Freshwater Biology*, *48*(5), 912–927. https://doi.org/10.1046/j.1365-2427.2003.01056.x

Di Prinzio, M., Castellarin, A., & Toth, E. (2011). Data-driven catchment classification: Application to the pub problem. *Hydrology and Earth System Sciences*, *15*(6), 1921–1935. https://doi.org/10.5194/hess-15-1921-2011

Eaton, B., & Moore, R. D. (2010). Regional hydrology. In R. G. Pike, T. E. Redding, R. D. Moore, R. D Winker, & K. D. Bladon (Eds.), *Compendium of forest hydrology and geomorphology in British Columbia*. Retrieved From www.for.gov.bc.ca/hfd/pubs/Docs/Lmh/Lmh66.htm

Edwards, R. T., D'Amore, D. V., Biles, F. E., Fellman, J. B., Hood, E. W., Trubilowicz, J. W., & Floyd, W. C. (2021). Riverine dissolved organic carbon and freshwater export in the Eastern Gulf of Alaska. *Journal of Geophysical Research: Biogeosciences*, *126*(1), 1–16. https://doi.org/10.1029/2020jg005725

Edwards, R. T., D'Amore, D. V., Norberg, E., & Biles, F. (2013). Riparian ecology, climate change, and management in North Pacific coastal rainforests. In G. Orians, & J. W. Schoen (Eds.), *North Pacific temperate rainforests: Ecology & conservation* (pp. 43–72). University of Washington Press.

Environment and Climate Change Canada. (2019). *Water quality data from Pacific coast stations [Pacific Data for Ian.xlsx]*. Provided by Ayisha Yeow.

Falcone, J. (2011). *GAGES-II: Geospatial attributes of Gages for evaluating streamflow. Vector digital data*. U.S. Geological Survey. Retrieved From https://water.usgs.gov/GIS/metadata/usgswrd/XML/gagesII_Sept2011.xml

Fellman, J. B., D'Amore, D. V., Hood, E., & Cunningham, P. (2017). Vulnerability of wetland soil carbon stocks to climate warming in the perhumid coastal temperate rainforest. *Biogeochemistry*, *133*(2), 165–179. https://doi.org/10.1007/s10533-017-0324-y

Fellman, J. B., Hood, E., Edwards, R. T., & D'Amore, D. V. (2009). Changes in the concentration, biodegradability, and fluorescent properties of dissolved organic matter during stormflows in coastal temperate watersheds. *Journal of Geophysical Research: Biogeosciences*, *114*(1), 1–14. https://doi.org/10.1029/2008jg000790

Fellman, J. B., Hood, E., Spencer, R. G. M., Stubbins, A., & Raymond, P. A. (2014). Watershed glacier coverage influences dissolved organic matter biogeochemistry in coastal watersheds of Southeast Alaska. *Ecosystems*, *17*, 1014–1025. https://doi.org/10.1007/s10021-014-9777-1

Fleming, S. W. (2005). Comparative analysis of glacial and nival streamflow regimes with implications for lotic habitat quantity and fish species richness. *River Research and Applications*, *21*(4), 363–379. https://doi.org/10.1002/rra.810

Fleming, S. W., Whitfield, P. H., Moore, R. D., & Quilty, E. J. (2007). Regime-dependent streamflow sensitivities to Pacific climate modes cross the Georgia–Puget transboundary ecoregion. *Hydrological Processes*, *21*, 3264–3287. https://doi.org/10.1002/hyp.6544

Gibson, J. J., Price, J. S., Aravena, R., Fitzgerald, D. F., & Maloney, D. (2000). Runoff generation in a hypermaritime bog-forest upland. *Hydrological Processes*, *2730*, 2711–2730. https://doi.org/10.1002/1099-1085(20001030)14:15<2711::aid-hyp88>3.0.co;2-2

Giesbrecht, I. J. W., Tank, S. E., Frazer, G. W., Hood, E., Gonzalez Arriola, S. G., Butman, D. E., et al. (2022). *Data from: Watershed classification predicts streamflow regime and organic carbon dynamics in the Northeast Pacific Coastal Temperate Rainforest*. https://doi.org/10.5061/dryad.05qfttf2q

Gómez-Gener, L., Hotchkiss, E. R., Laudon, H., & Sponseller, R. A. (2021). Integrating discharge-concentration dynamics across carbon forms in a Boreal landscape. *Water Resources Research*, *57*(8), 1–18. https://doi.org/10.1029/2020wr028806

Goñi, M. A., Hatten, J. A., Wheatcroft, R. A., & Borgeld, J. C. (2013). Particulate organic matter export by two contrasting small mountainous rivers from the Pacific Northwest, U.S.A. *Journal of Geophysical Research: Biogeosciences*, *118*, 112–134. https://doi.org/10.1002/jgrg.20024

Gonzalez Arriola, S., Giesbrecht, I. J. W., Biles, F. E., & D'Amore, D. V. (2018). *Watersheds of the northern Pacific coastal temperate rainforest margin*. Hakai Institute Data Package. https://doi.org/10.21966/1.715755

Greene, S., Johnes, P. J., Bloomfield, J. P., Reaney, S. M., Lawley, R., Elkhatib, Y., et al. (2015). A geospatial framework to support integrated biogeochemical modelling in the United Kingdom. *Environmental Modelling and Software*, *68*, 219–232. https://doi.org/10.1016/j.envsoft.2015.02.012

Gregorutti, B., Bertrand, M., & Saint-Pierre, P. (2017). Correlation and variable importance in random forests. *Statistics and Computing*, *27*, 659–678. https://doi.org/10.1007/s11222-016-9646-1

Guyon, I., Weston, J., Barnhill, S., & Vapnik, V. (2002). Gene selection for cancer classification using support vector machines. *Machine Learning*, *46*(1), 389–422. https://doi.org/10.1023/a:1012487302797

Hastie, T., Tibshirani, R., & Friedman, J. (2009). *The elements of statistical learning: Data mining, inference, and prediction*. Springer. https://doi.org/10.1007/b94608

Higgins, J. V., Bryer, M. T., Khoury, M. L., & Fitzhugh, T. W. (2005). A freshwater classification approach for biodiversity conservation planning. *Conservation Biology*, *19*(2), 432–445. https://doi.org/10.1111/j.1523-1739.2005.00504.x

Hitchcock, J. N., Mitrovic, S. M., Hadwen, W. L., Roelke, D. L., Growns, I. O., & Rohlfs, A. M. (2016). Terrestrial dissolved organic carbon subsidizes estuarine zooplankton: An in situ mesocosm study. *Limnology and Oceanography*, *61*(1), 254–267. https://doi.org/10.1002/lno.10207

Hodson, A., Mumford, P., & Lister, D. (2004). Suspended sediment and phosphorous in proglacial rivers: Bioavailability and potential impacts upon the P status of ice-marginal receiving waters. *Hydrological Processes*, *18*(13), 2409–2422. https://doi.org/10.1002/hyp.1471

Hood, E., & Berner, L. (2009). Effects of changing glacial coverage on the physical and biogeochemical properties of coastal streams in southeastern Alaska. *Journal of Geophysical Research*, *114*, 1–10. https://doi.org/10.1029/2009jg000971

Hood, E., Fellman, J., Spencer, R. G. M., Hernes, P. J., Edwards, R., D'Amore, D., & Scott, D. (2009). Glaciers as a source of ancient and labile organic matter to the marine environment. *Nature*, *462*(7276), 1044–1047. https://doi.org/10.1038/nature08580

Hood, E., Fellman, J. B., & Spencer, R. G. M. (2020). Glacier loss impacts riverine organic carbon transport to the ocean. *Geophysical Research Letters*, *47*(19), 1–9. https://doi.org/10.1029/2020gl089804

Hood, E., Gooseff, M. N., & Johnson, S. L. (2006). Changes in the character of stream water dissolved organic carbon during flushing in three small watersheds, Oregon. *Journal of Geophysical Research*, *111*(1), 1–8. https://doi.org/10.1029/2005jg000082

Hoos, A. B., & McMahon, G. (2009). Spatial analysis of instream nitrogen loads and factors controlling nitrogen delivery to streams in the southeastern United States using spatially referenced regression on watershed attributes (SPARROW) and regional classification frameworks. *Hydrological Processes*, *23*, 2275–2294. https://doi.org/10.1002/hyp.7323

Howe, E., Simenstad, C. A., & Ogston, A. (2017). Detrital shadows: Estuarine food web connectivity depends on fluvial influence and consumer feeding mode. *Ecological Applications*, *27*(7), 2170–2193. https://doi.org/10.1002/eap.1600

Ishwaran, H. (2007). Variable importance in binary regression trees and forests. *Electronic Journal of Statistics*, *1*, 519–537. https://doi.org/10.1214/07-ejs039

Jansen, N., Hartmann, J., Lauerwald, R., Dürr, H. H., Kempe, S., Loos, S., & Middelkoop, H. (2010). Dissolved silica mobilization in the conterminous USA. *Chemical Geology*, *270*(1–4), 90–109. https://doi.org/10.1016/j.chemgeo.2009.11.008

Kennard, M. J., Mackay, S. J., Pusey, B. J., Olden, J. D., & Marsh, N. (2010). Quantifying uncertainty in estimation of hydrologic metrics for ecohydrological studies. *River Research and Applications*, *26*, 137–156. https://doi.org/10.1111/j.1752-0118.2010.01202.x

Kritzberg, E. S., Villanueva, A. B., Jung, M., & Reader, H. E. (2014). Importance of boreal rivers in providing iron to marine waters. *PLoS One*, *9*(9), e107500. https://doi.org/10.1371/journal.pone.0107500

Lajtha, K., & Jones, J. (2018). Forest harvest legacies control dissolved organic carbon export in small watersheds, western Oregon. *Biogeochemistry*, *140*(3), 299–315. https://doi.org/10.1007/s10533-018-0493-3

Lane, B. A., Sandoval-Solis, S., Stein, E. D., Yarnell, S. M., Pasternack, G. B., & Dahlke, H. E. (2018). Beyond metrics? The role of hydrologic baseline archetypes in environmental water management. *Environmental Management*, *62*(4), 678–693. https://doi.org/10.1007/s00267-018-1077-7

Larsen, A. S., O'Donnell, J. A., Schmidt, J. H., Kristenson, H. J., & Swanson, D. K. (2017). Physical and chemical characteristics of lakes across heterogeneous landscapes in arctic and subarctic Alaska. *Journal of Geophysical Research: Biogeosciences*, *122*, 989–1008. https://doi.org/10.1002/2016jg003729

K. Lertzman, & A. MacKinnon, (2013). Why watersheds: Evaluating the protection of undeveloped watersheds as a conservation strategy in Northwestern North America. In Orians, G. H., & Schoen, J. W. (Eds.), *North Pacific temperate rainforests: Ecology & conservation* (pp. 189–226). University of Washington Press.

Li, L., Sullivan, P. L., Benettin, P., Cirpka, O. A., Bishop, K., Brantley, S. L., & Kirchner, J. W. (2021). Toward catchment hydro-biogeochemical theories. *Wiley Interdisciplinary Reviews: Water*, *8*(1), 1–31. https://doi.org/10.1002/wat2.1495

Littell, J. S., McAfee, S. A., & Hayward, G. D. (2018). Alaska snowpack response to climate change: Statewide snowfall equivalent and snowpack water scenarios. *Water*, *10*(5). https://doi.org/10.3390/w10050668

Lyons, W. B., Nezat, C. A., Carey, A. E., & Hicks, D. M. (2002). Organic carbon fluxes to the ocean from high-standing islands. *Geology*, *30*(5), 443–446. https://doi.org/10.1130/0091-7613(2002)030<0443:ocftto>2.0.co;2

Martin, S. L., Soranno, P. A., Bremigan, M. T., & Cheruvelil, K. S. (2011). Comparing hydrogeomorphic approaches to lake classification. *Environmental Management*, *48*(5), 957–974. https://doi.org/10.1007/s00267-011-9740-2

Mayorga, E., Seitzinger, S. P., Harrison, J. A., Dumont, E., Beusen, A. H. W., Bouwman, A. F., et al. (2010). Global Nutrient Export from WaterSheds 2 (NEWS 2): Model development and implementation. *Environmental Modelling and Software*, *25*(7), 837–853. https://doi.org/10.1016/j.envsoft.2010.01.007

McClain, M. E., Boyer, E. W., Dent, C. L., Gergel, S. E., Grimm, N. B., Groffman, P. M., et al. (2003). Biogeochemical hot spots and hot moments at the interface of terrestrial and aquatic ecosystems. *Ecosystems*, *6*, 301–312. https://doi.org/10.1007/s10021-003-0161-9

McClelland, J. W., Tank, S. E., Spencer, R. G. M., & Shiklomanov, A. I. (2015). Coordination and sustainability of river observing activities in the Arctic. *Arctic*, *68*, 59–68. https://doi.org/10.14430/arctic4448

McDonnell, J. J., & Woods, R. (2004). On the need for catchment classification. *Journal of Hydrology*, *299*(1–2), 2–3. https://doi.org/10.1016/s0022-1694(04)00421-4

McManamay, R. A., Bevelhimer, M. S., & Kao, S.-C. (2014). Updating the US hydrologic classification: An approach to clustering and stratifying ecohydrologic data. *Ecohydrology*, *7*(3), 903–926. https://doi.org/10.1002/eco.1410

McMillan, H. (2020). Linking hydrologic signatures to hydrologic processes: A review. *Hydrological Processes*, *34*(6), 1393–1409. https://doi.org/10.1002/hyp.13632

McNicol, G., Bulmer, C., D'Amore, D., Sanborn, P., Saunders, S., Giesbrecht, I. J. W., & Buma, B. (2019). Large, climate-sensitive soil carbon stocks mapped with pedology-informed machine learning in the North Pacific coastal temperate rainforest. *Environmental Research Letters*, *14*(1), 14004. https://doi.org/10.1088/1748-9326/aaed52

Melles, S. J., Jones, N. E., & Schmidt, B. (2012). Review of theoretical developments in stream ecology and their influence on stream classification and conservation planning. *Freshwater Biology*, *57*(3), 415–434. https://doi.org/10.1111/j.1365-2427.2011.02716.x

Melles, S. J., Jones, N. E., & Schmidt, B. J. (2014). Evaluation of current approaches to stream classification and a heuristic guide to developing classifications of integrated aquatic networks. *Environmental Management*, *53*(3), 549–566. https://doi.org/10.1007/s00267-014-0231-0

Menounos, B., Osborn, G., Clague, J. J., & Luckman, B. H. (2009). Latest Pleistocene and Holocene glacier fluctuations in western Canada. *Quaternary Science Reviews*, *28*, 2049–2074. https://doi.org/10.1016/j.quascirev.2008.10.018

Milliman, J. D., & Farnsworth, K. L. (2011). *River discharge to the coastal ocean: A global synthesis*. Cambridge University Press. https://doi.org/10.1017/CBO9780511781247

Milliman, J. D., & Syvitski, J. P. M. (1992). Geomorphic/tectonic control of sediment discharge to the ocean: The importance of small mountainous rivers. *Journal of Geology*, *100*(5), 525–544. https://doi.org/10.1086/629606

Milner, A. M., Khamis, K., Battin, T. J., Brittain, J. E., Barrand, N. E., Füreder, L., et al. (2017). Glacier shrinkage driving global changes in downstream systems. *Proceedings of the National Academy of Sciences of the United States of America*, *114*(37), 9770–9778. https://doi.org/10.1073/pnas.1619807114

Momen, B., & Zehr, J. P. (1998). Watershed classification by discriminant analyses of lakewater-chemistry and terrestrial characteristics. *Ecological Applications*, *8*(2), 497–507. https://doi.org/10.1890/1051-0761(1998)008[0497:wcbdao]2.0.co;2

Moore, R. D., Fleming, S. W., Menounos, B., Wheate, R., Fountain, A., Stahl, K., et al. (2009). Glacier change in Western North America: Influences on hydrology, geomorphic hazards and water quality. *Hydrological Processes*, *23*, 42–61. https://doi.org/10.1002/hyp.7162

Morrison, J., Foreman, M. G. G., & Masson, D. (2012). A method for estimating monthly freshwater discharge affecting British Columbia coastal waters. *Atmosphere-Ocean*, *50*(1), 1–8. https://doi.org/10.1080/07055900.2011.637667

Mosavi, A., Golshan, M., Choubin, B., & Ziegler, A. D. (2021). Fuzzy clustering and distributed model for streamflow estimation in ungauged watersheds. *Scientific Reports*, *1–14*. https://doi.org/10.1038/s41598-021-87691-0

Mosher, J. J., Klein, G. C., Marshall, A. G., & Findlay, R. H. (2010). Influence of bedrock geology on dissolved organic matter quality in stream water. *Organic Geochemistry*, *41*(11), 1177–1188. https://doi.org/10.1016/j.orggeochem.2010.08.004

Mulholland, P. J. (2003). Large-scale patterns in dissolved organic carbon concentration, flux, and sources. In S. E. G. Findlay, & R. L. Sinsabaugh (Eds.), *Aquatic ecosystems: Interactivity of dissolved organic matter* (pp. 139–159). Academic Press. https://doi.org/10.1016/b978-012256371-3/50007-x

Neal, E. G., Hood, E., & Smikrud, K. (2010). Contribution of glacier runoff to freshwater discharge into the Gulf of Alaska. *Geophysical Research Letters*, *37*(6), 1–5. https://doi.org/10.1029/2010gl042385

Nicodemus, K. K., Malley, J. D., Strobl, C., & Ziegler, A. (2010). The behaviour of random forest permutation-based variable importance measures under predictor correlation. *BMC Bioinformatics*, *11*(110), 1–13. https://doi.org/10.1186/1471-2105-11-110

Obedzinski, M., Nossaman Pierce, S., Horton, G. E., & Deitch, M. J. (2018). Effects of flow-related variables on oversummer survival of juvenile Coho salmon in intermittent streams. *Transactions of the American Fisheries Society*, *147*(3), 588–605. https://doi.org/10.1002/tafs.10057

Olden, J. D., Kennard, M. J., & Pusey, B. J. (2012). A framework for hydrologic classification with a review of methodologies and applications in ecohydrology. *Ecohydrology*, *5*(4), 503–518. https://doi.org/10.1002/eco.251

Oliver, A. A., Spencer, R. G. M., Deas, M. L., & Dahlgren, R. A. (2016). Impact of seasonality and anthropogenic impoundments on dissolved organic matter dynamics in the Klamath River (Oregon/California, USA). *Journal of Geophysical Research: Biogeosciences*, *121*(7), 1946–1958. https://doi.org/10.1002/2016jg003497

Oliver, A. A., Tank, S. E., Giesbrecht, I., Korver, M. C., Floyd, W. C., Sanborn, P., et al. (2017). A global hotspot for dissolved organic carbon in hypermaritime watersheds of coastal British Columbia. *Biogeosciences*, *14*(15), 3743–3762. https://doi.org/10.5194/bg-14-3743-2017

O'Neel, S., Hood, E., Bidlack, A. L., Fleming, S. W., Arimitsu, M. L., Arendt, A., & Pyare, S. (2015). Icefield-to-ocean linkages across the northern pacific coastal temperate rainforest ecosystem. *BioScience*, *65*(5), 499–512. https://doi.org/10.1093/biosci/biv027

Ouellet Dallaire, C., Lehner, B., & Creed, I. (2020). Multidisciplinary classification of Canadian river reaches to support the sustainable management of freshwater systems. *Canadian Journal of Fisheries and Aquatic Sciences*, *77*(2), 326–341. https://doi.org/10.1139/cjfas-2018-0284

Ouellet Dallaire, C., Lehner, B., Sayre, R., & Thieme, M. (2019). A multidisciplinary framework to derive global river reach classifications at high spatial resolution. *Environmental Research Letters*, *14*(2). https://doi.org/10.1088/1748-9326/aad8e9

Peredo-Parada, M., Martínez-Capel, F., Quevedo, D. I., & Hernández-Mascarell, A. B. (2011). Implementation of an eco-hydrological classification in Chilean rivers. *Gayana*, *75*(1), 26–38. https://doi.org/10.4067/s0717-65382011000100003

Phillips, A. K., & Cowling, S. A. (2019). Biotic and abiotic controls on watershed Si cycling and river Si yield in western Canada. *Biogeochemistry*, *143*(2), 221–237. https://doi.org/10.1007/s10533-019-00557-6

Poff, N. L. (1996). A hydrogeography of unregulated streams in the United States and an examination of scale-dependence in some hydrological descriptors. *Freshwater Biology*, *36*(1), 71–79. https://doi.org/10.1046/j.1365-2427.1996.00073.x

Poor, C. J., McDonnell, J. J., & Bolte, J. (2008). Testing the hydrological landscape unit classification system and other terrain analysis measures for predicting low-flow nitrate and chloride in watersheds. *Environmental Management*, *42*(5), 877–893. https://doi.org/10.1007/s00267-008-9168-5

Radić, V., Cannon, A. J., Menounos, B., & Gi, N. (2015). Future changes in autumn atmospheric river events in British Columbia, Canada, as projected by CMIP5 global climate models. *Journal of Geophysical Research: Atmospheres*, *120*, 9279–9302. https://doi.org/10.1002/2015JD023279

Regnier, P., Friedlingstein, P., Ciais, P., Mackenzie, F. T., Gruber, N., Janssens, I. A., et al. (2013). Anthropogenic perturbation of the carbon fluxes from land to ocean. *Nature Geoscience*, *6*(8), 597–607. https://doi.org/10.1038/ngeo1830

Reidy Liermann, C. A., Olden, J. D., Beechie, T. J., Kennard, M. J., Skidmore, P. B., Konrad, C. P., & Imaki, H. (2012). Hydrogeomorphic classification of Washington State rivers to support emerging environmental flow management strategies. *River Research and Applications*, *28*, 1340–1358. https://doi.org/10.1002/rra.1541

RGI Consortium. (2015). *Global land ice measurements from space*. Digital Media. https://doi.org/10.7265/N5-RGI-50

Roden, G. I. (1967). On river discharge into the northeastern Pacific Ocean and the Bering Sea. *Journal of Geophysical Research*, *72*(22), 5613–5629. https://doi.org/10.1029/jz072i022p05613

Rolls, R. J., Leigh, C., & Sheldon, F. (2012). Mechanistic effects of low-flow hydrology on riverine ecosystems: Ecological principles and consequences of alteration. *Freshwater Science*, *31*(4), 1163–1186. https://doi.org/10.1899/12-002.1

Royer, T. C. (1982). Coastal fresh water discharge in the northeast Pacific. *Journal of Geophysical Research*, *87*(C3), 2017–2021. https://doi.org/10.1029/jc087ic03p02017

Salkfield, T., Walton, A., & Mackenzie, W. (2016). *Biogeoclimatic ecosystem classification map*. Ministry of Forests, Lands, Natural Resource Operations and Rural Development—Forest Analysis and Inventory. Retrieved from https://catalogue.data.gov.bc.ca/dataset/bec-map

Sanborn, S. C., & Bledsoe, B. P. (2006). Predicting streamflow regime metrics for ungauged streamsin Colorado, Washington, and Oregon. *Journal of Hydrology*, *325*(1–4), 241–261. https://doi.org/10.1016/j.jhydrol.2005.10.018

Schlesinger, W. H. (1997). *Biogeochemistry: An analysis of global change* (2nd ed.). Academic Press.

Schnorbus, M., Werner, A., & Bennett, K. (2014). Impacts of climate change in three hydrologic regimes in British Columbia, Canada. *Hydrological Processes*, *28*(3), 1170–1189. https://doi.org/10.1002/hyp.9661

Schroth, A. W., Crusius, J., Chever, F., Bostick, B. C., & Rouxel, O. J. (2011). Glacial influence on the geochemistry of riverine iron fluxes to the Gulf of Alaska and effects of deglaciation. *Geophysical Research Letters*, *38*, L16605. https://doi.org/10.1029/2011gl048367

Sergeant, C. J., Bellmore, J. R., McConnell, C., & Moore, J. W. (2017). High salmon density and low discharge create periodic hypoxia in coastal rivers. *Ecosphere*, *8*(6). https://doi.org/10.1002/ecs2.1846

Sergeant, C. J., Falke, J. A., Bellmore, R. A., Bellmore, J. R., & Crumley, R. L. (2020). A classification of streamflow patterns across the coastal Gulf of Alaska. *Water Resources Research*, *56*(2), 1–17. https://doi.org/10.1029/2019wr026127

Shanley, C. S., Pyare, S., Goldstein, M. I., Alaback, P. B., Albert, D. M., Beier, C. M., et al. (2015). Climate change implications in the northern coastal temperate rainforest of North America. *Climatic Change*, *130*(2), 155–170. https://doi.org/10.1007/s10584-015-1355-9

Sivakumar, B. (2004). Dominant processes concept in hydrology: Moving forward. *Hydrological Processes*, *18*(12), 2349–2353. https://doi.org/10.1002/hyp.5606

Sivakumar, B., Singh, V. P., Berndtsson, R., & Khan, S. K. (2015). Catchment classification framework in hydrology: Challenges and directions. *Journal of Hydrologic Engineering*, *20*(1), 1–12. https://doi.org/10.1061/(asce)he.1943-5584.0000837

Smith, T., Marshall, L., & McGlynn, B. (2018). Typecasting catchments: Classification, directionality, and the pursuit of universality. *Advances in Water Resources*, *112*, 245–253. https://doi.org/10.1016/j.advwatres.2017.12.020

Snelder, T. H., & Biggs, B. J. F. (2002). Multiscale river environment classification for water resources management. *Journal of the American Water Resources Association*, *38*(5), 1225–1239. https://doi.org/10.1111/j.1752-1688.2002.tb04344.x

Snelder, T. H., & Hughey, K. F. D. (2005). The use of an ecologic classification to improve water resource planning in New Zealand. *Environmental Management*, *36*(5), 741–756. https://doi.org/10.1007/s00267-004-0324-2

Soranno, P. A., Cheruvelil, K. S., Webster, K. E., Bremigan, M. T., Wagner, T., & Stow, C. A. (2010). Using landscape limnology to classify freshwater ecosystems for multi-ecosystem management and conservation. *BioScience*, *60*(6), 440–454. https://doi.org/10.1525/bio.2010.60.6.8

Stackpoole, S. M., Butman, D. E., Clow, D. W., Verdin, K. L., Gaglioti, B. V., Genet, H., & Striegl, R. G. (2017). Inland waters and their role in the carbon cycle of Alaska. *Ecological Applications*, *27*(5), 1403–1420. https://doi.org/10.1002/eap.1552

Stahl, K., & Moore, R. D. (2006). Influence of watershed glacier coverage on summer streamflow in British Columbia, Canada. *Water Resources Research*, *42*, 1–5. https://doi.org/10.1029/2006wr005022

St. Pierre, K., Hunt, B., Tank, S., Giesbrecht, I., Korver, M., Floyd, W., et al. (2021). Rain-fed streams dilute inorganic nutrients but subsidise organic-matter-associated nutrients in coastal waters of the northeast Pacific Ocean. *Biogeosciences*, *18*, 3029–3052. https://doi.org/10.5194/bg-18-3029-2021

St. Pierre, K. A., Oliver, A. A., Tank, S. E., Hunt, B. P. V, Giesbrecht, I. J. W., Kellogg, C. T. E., et al. (2020). Terrestrial exports of dissolved and particulate organic carbon affect nearshore ecosystems of the Pacific coastal temperate rainforest. *Limnology & Oceanography*, *65*, 2657–2675. https://doi.org/10.1002/lno.11538

Sugai, S. F., & Burrell, D. C. (1984). Transport of dissolved organic carbon, nutrients, and trace metals from the Wilson and Blossom rivers to Smeaton Bay, southeast Alaska. *Canadian Journal of Fisheries and Aquatic Sciences*, *41*(1), 180–190. https://doi.org/10.1139/f84-019

Syvitski, J. P. M., Vörösmarty, C. J., Kettner, A. J., & Green, P. (2005). Impact of humans on the flux of terrestrial sediment to the global coastal ocean. *Science*, *308*, 376–381. https://doi.org/10.1126/science.1109454

Tank, S. E., Giesbrecht, I. J. W., Fedje, B., Myers, E., Quayle, L., Desmarais, I., et al. (2020). *Biogeochemical sampling of streams in the Kwakshua watersheds of Calvert and Hecate islands, BC: 2013-2019. Version 1.0*. Hakai Institute Data Package. https://doi.org/10.21966/7qnv-6y88

Tank, S. E., Raymond, P. A., Striegl, R. G., McClelland, J. W., Holmes, R. M., Fiske, G. J., & Peterson, B. J. (2012). A land-to-ocean perspective on the magnitude, source and implication of DIC flux from major Arctic rivers to the Arctic Ocean. *Global Biogeochemical Cycles*, *26*(4), 1–15. https://doi.org/10.1029/2011gb004192

Trubilowicz, J. W., Moore, R. D., & Buttle, J. M. (2013). Prediction of stream-flow regime using ecological classification zones. *Hydrological Processes*, *27*(13), 1935–1944. https://doi.org/10.1002/hyp.9874

Voss, B. M., Peucker-Ehrenbrink, B., Eglinton, T. I., Spencer, R. G. M., Bulygina, E., Galy, V., et al. (2015). Seasonal hydrology drives rapid shifts in the flux and composition of dissolved and particulate organic carbon and major and trace ions in the Fraser River, Canada. *Biogeosciences*, *12*, 5597–5618. https://doi.org/10.5194/bg-12-5597-2015

Wade, N. L., Martin, J., & Whitfield, P. H. (2001). Hydrologic and climatic zonation of Georgia Basin, British Columbia. *Canadian Water Resources Journal*, *26*(1), 43–70. https://doi.org/10.4296/cwrj2601043

Wang, J., Jin, M., Musgrave, D. L., & Ikeda, M. (2004). A hydrological digital elevation model for freshwater discharge into the Gulf of Alaska. *Journal of Geophysical Research*, *109*(7), 1–15. https://doi.org/10.1029/2002jc001430

Wang, T., Hamann, A., Spittlehouse, D., & Carroll, C. (2016). Locally downscaled and spatially customizable climate data for historical and future periods for North America. *PLoS One*, *11*(6), 1–17. https://doi.org/10.1371/journal.pone.0156720

Wetz, M. S., Hales, B., Chase, Z., Wheeler, P. A., & Whitney, M. M. (2006). Riverine input of macronutrients, iron, and organic matter to the coastal ocean off Oregon, U.S.A., during the winter. *Limnology and Oceanography*, *51*(5), 2221–2231. https://doi.org/10.4319/lo.2006.51.5.2221

Wheatcroft, R. A., Goñi, M. A., Hatten, J. A., Pasternack, G. B., & Warrick, J. A. (2010). The role of effective discharge in the ocean delivery of particulate organic carbon by small, mountainous river systems. *Limnology and Oceanography*, *55*(1), 161–171. https://doi.org/10.4319/lo.2010.55.1.0161

Winfree, M. M., Hood, E., Stuefer, S. L., Schindler, D. E., Cline, T. J., Arp, C. D., & Pyare, S. (2018). Landcover and geomorphology influence streamwater temperature sensitivity in salmon bearing watersheds in Southeast Alaska. *Environmental Research Letters*, *13*(6). https://doi.org/10.1088/1748-9326/aac4c0

Winterdahl, M., Erlandsson, M., Futter, M. N., Weyhenmeyer, G. A., & Bishop, K. (2014). Intra-annual variability of organic carbon concentrations in running waters: Drivers along a climatic gradient. *Global Biogeochemical Cycles*, *28*, 451–464. https://doi.org/10.1002/2013gb004770

Wolf, E. C., Mitchell, A. P., & Schoonmaker, P. K. (1995). *The Rain Forests of Home: An Atlas of People and Place* (Vol. 31). Interrain. Retrieved from http://www.ecotrust.org/publications/rain_forests_atlas.html

Wolfe, J. D., Shook, K. R., Spence, C., & Whitfield, C. J. (2019). A watershed classification approach that looks beyond hydrology: Application to a semi-arid, agricultural region in Canada. *Hydrology and Earth System Sciences*, *23*(9), 3945–3967. https://doi.org/10.5194/hess-23-3945-2019

Wolock, D. M., Winter, T. C., & McMahon, G. (2004). Delineation and evaluation of hydrologic-landscape regions in the United States using geographic information system tools and multivariate statistical analyses. *Environmental Management*, *34*, 71–88. https://doi.org/10.1007/s00267-003-5077-9

Xenopoulos, M. A., Downing, J. A., Kumar, M. D., Menden-Deuer, S., & Voss, M. (2017). Headwaters to oceans: Ecological and biogeochemical contrasts across the aquatic continuum. *Limnology and Oceanography*, *62*. S3–S14. https://doi.org/10.1002/lno.10721

Yu, S., Xu, Z., Liu, X., Dou, T., & Xu, C. (2015). Identifying and validating freshwater ecoregions in Jinan City, China. *Journal of Hydrology*, *528*, 763–772. https://doi.org/10.1016/j.jhydrol.2015.07.010

Zarnetske, J. P., Bouda, M., Abbott, B. W., Saiers, J., & Raymond, P. A. (2018). Generality of hydrologic transport limitation of watershed organic carbon flux across ecoregions of the United States. *Geophysical Research Letters*, *45*(21), 11702–11711. https://doi.org/10.1029/2018gl080005

References From the Supporting Information

Lehner, B., Verdin, K., & Jarvis, A. (2008). New global hydrography derived from spaceborne elevation data. *Eos*, *89*(10), 93–94. https://doi.org/10.1029/2008eo100001

Simard, M., Pinto, N., Fisher, J. B., & Baccini, A. (2011). Mapping forest canopy height globally with spaceborne lidar. *Journal of Geophysical Research*, *116*(4), 1–12. https://doi.org/10.1029/2011jg001708

Sobek, S., Tranvik, L. J., Prairie, Y. T., Kortelainen, P., & Cole, J. J. (2007). Patterns and regulation of dissolved organic carbon: An analysis of 7,500 widely distributed lakes. *Limnology and Oceanography*, *52*(3), 1208–1219. https://doi.org/10.4319/lo.2007.52.3.1208